

Applied Spectroscopy Reviews



ISSN: 0570-4928 (Print) 1520-569X (Online) Journal homepage: http://www.tandfonline.com/loi/laps20

Plasmonic nanoparticles and their analytical applications: A review

Jyoti Boken, Parul Khurana, Sheenam Thatai, Dinesh Kumar & Surendra Prasad

To cite this article: Jyoti Boken, Parul Khurana, Sheenam Thatai, Dinesh Kumar & Surendra Prasad (2017) Plasmonic nanoparticles and their analytical applications: A review, Applied Spectroscopy Reviews, 52:9, 774-820, DOI: <u>10.1080/05704928.2017.1312427</u>

To link to this article: https://doi.org/10.1080/05704928.2017.1312427

	Accepted author version posted online: 31 Mar 2017. Published online: 19 Apr 2017.
	Submit your article to this journal 🗷
ılıl	Article views: 364
Q	View related articles ☑
CrossMark	View Crossmark data ☑
4	Citing articles: 3 View citing articles 🗹





Plasmonic nanoparticles and their analytical applications: A review

Jyoti Boken^a, Parul Khurana^b, Sheenam Thatai^c, Dinesh Kumar^d, and Surendra Prasad^e

^aDepartment of Physics, Banasthali University, Banasthali, Rajasthan, India; ^bDepartment of Chemistry, Guru Nanak Khalsa College of Arts, Science & Commerce, Matunga East, Mumbai, India; ^cDepartment of Chemistry, Amity Institute of Applied Sciences, Amity University, Noida, India; ^dSchool of Chemical Sciences, Central University of Gujarat, Gandhinagar, Gujarat, India; ^eSchool of Biological and Chemical Sciences, Faculty of Science, Technology and Environment, The University of the South Pacific, Suva, Fiji

ABSTRACT

Plasmonic nanoparticles (NPs) have been reviewed herein for their fascinating optical properties in a wide spectral range and for their various applications. The surface plasmon resonance (SPR) bands of metal NPs can be tuned from visible to near infrared region by varying the shape of the metal NPs. As a result, the tuning of the SPR band over a spectral range is possible by making plasmonic NPs of different shapes. This review emphasizes fundamental studies of plasmonic NPs and nanocomposites with well-defined and controlled shapes that have several analytical applications such as molecular detection and determination in different fields. This review describes how oxidative etching and kinetic control can be utilized to manipulate the shape and optical properties of NPs. This review also describes the specific examples of the sensing applications of the localized surface plasmon resonance studies in which the researchers use both wavelength shift and surface-enhanced Raman scattering sensing to detect the molecules of chemical and biological relevance. The review ends with a perspective of the field, identifying the main challenges to be overcome and suggesting areas where the most promising developments are likely to happen in future.

KEYWORDS

Nanoparticles; shapecontrolled synthesis; localized surface plasmon resonance; surface-enhanced Raman scattering; tipenhanced Raman scattering

Abbreviations

AA Ascorbic acid

AFM Atomic force microscopy

APTES 3-Aminopropyltriethoxysilane

CTAB Hexadecyltrimethylammonium bromide

DDA Discrete dipole approximation

DNA Deoxyribonucleic acid

EDX Energy dispersive X-ray spectroscopy

EuTDPA Tris(dibenzoylmethane) mono (5-amino phenanthroline) europium

CONTACT Dinesh Kumar or Surendra Prasad Schoudhary2002@yahoo.com or prasad_su@usp.ac.fj School of Chemical Sciences, Central University of Gujarat, Gandhinagar 382030, Gujarat India; or School of Biological and Chemical Sciences, Faculty of Science, Technology and Environment, The University of the South Pacific, Private Mail Bag, Suva Fiji.

Color versions of one or more figures in this article are available online at www.tanfonline.com/laps.



HAuCl₄ Tetrachloroauric acid

Irgacure 2959 1-[4-(2-hydroxyethoxy) phenyl]-2-hydroxy-2-methyl-1-propan-1-one

LSPR Localized surface plasmon resonance

MWCNTs Multi-walled carbon nanotubes

NaBH₄ Sodium borohydride NaBr Sodium bromide

NCs Nanocomposites

NPs Nanoparticles

NRs Nanorods

PTFE Polytetrafluorethylene

PVP Polyvinylpyrrolidone PVP Polyvinylpyrrolidone

RNA Ribonucleic acid

SDS Sodium dodecyl sulfate

SERS Surface-enhanced Raman scattering

SPPs Surface plasmon polaritons SPR Surface plasmon resonance

TDAB Tetradodecylammoniumbromide TEM Transmission electron microscopy

TEOS Tetraethylorthosilicate

Introduction

Nanoparticles (NPs), notable for their small size, high surface area to volume ratios, and strong adsorption capacity, have been the subject of great interest in analytical chemistry (1, 2). Metal NPs-based analytical techniques have become increasingly important in clinical, pharmaceutical, environmental, and food safety fields owing to their high sensitivity, wide linear range, and simple instrumentation, and thus over the past decade, NPs have been widely used for elemental detection and speciation (1, 2). Thus, metal nanostructures have gained considerable attention both fundamentally and technologically because of their many peculiar properties and functionalities compared to their bulk counterparts. One of the most important aspects of NPs is their optical properties. In the nanoscale domain, many metals like silver and gold exhibit strong absorption in the visible region. These optical properties of nanoscale metal particles depend on various parameters such as their dimensions (3), shapes (4), the composition of metal (5), optical properties, and surrounding medium of the particles (5-10). The optical properties of metal nanostructures are magnificent and therefore have enhanced a great deal of excitement in the last few years (1-3, 5-7, 9-11). The variations in color arise from changes in shape, size distribution, surrounding medium and high absorption, which promoted these materials as inorganic chromophores from visible to near infrared region. Owing to this researchers are prompted to find various applications of metal nanostructures as optical sensors and imaging agents (11-14). For example, nowadays nanomaterials are also recognized as excellent candidates to detect biological impurities, such as the presence of Escherichia coli in water (15, 16). Through this review, we attempt to show that NPs and core-shell nanocomposites (NCs), i.e., nanomaterials, have well been utilized as new generation water remediation materials (16).

Metal NPs play an important role in many different fields. For example, they can serve as a model system to experimentally probe the effects of quantum confinement on magnetic, electronic, and other relevant properties (17, 18). The metallic NPs have also been used in many areas such as catalysis (19), photography (20), biological labeling (2, 21), photonics (22), optoelectronics (23), information storage (24), and surface-enhanced Raman scattering (SERS) (25, 26).

Metallic NPs can be obtained by various synthetic routes such as electrochemical methods, decomposition of organometallic precursors, and reduction of metal salts in the presence of stabilizers or vapor deposition methods. Sometimes the presence of stabilizer is required to prevent the agglomeration of nanoclusters. In addition, the stabilizers play a crucial role in controlling both the shape and size of NPs (27).

NPs are complicated multi-electron systems where the confinement of electronic motion due to the reduction in size leads to fascinating effects, potentially tunable with particle size and shape. In addition, almost any shape can be produced. These different shaped nanostructures exhibit different absorption spectra or colors. More complex structures such as aggregates, nanocages, and nanoprism usually have more nondegenerate resonances and obtain broad absorption spectrum. It has been shown that due to lower symmetry of structures more nondegenerate modes are obtained (28).

These optical properties exhibited by metal NPs are due to the surface plasmon resonance (SPR), and correspond to the frequency of oscillation at which conduction electrons oscillates in response to the electrical field of the incident electromagnetic radiation. The surface plasmons are essentially electromagnetic waves trapped at the metal/dielectric interface due to the collective oscillations with the free electrons of the metal. This phenomenon was explained by Mie theory and is based on the Maxwell equation on scattering (14). Materials that possess negative real and positive imaginary dielectric constants are capable of supporting the SPR. This resonance is a coherent oscillation of the surface conduction electrons excited by electromagnetic radiation of light. Plasmonics is the study of these particular light interactions that have enabled various applications such as biological and chemical sensing (1, 2, 13, 25, 29-45), lithographic fabrication of the materials (20, 46-48), and surfaceenhanced spectroscopies (49-64). However, only gold, silver, and copper NPs exhibit plasmon resonance effects in the visible spectrum, giving rise to intense colored particles. It is due to the fact that resonance frequency of the SPR depends on the shape, size, and surrounding medium of the particles (3, 4, 8, 16, 65). Au and Ag NPs play a significant role in the visible region due to surface plasmon absorption and the surface accessibility for further functionalization (15, 16, 40, 66-68). These NPs are known for their interesting optical properties caused by plasmonic resonance with significant absorption and scattering at 530 nm and 400 nm for gold and silver, respectively. These NPs have been studied for various analytical, environmental, and medical applications such as laser biomedicine, laser-combined imaging, photothermal therapy, cancer research, biosensors, etc. (15, 16, 40, 66–71).

The optical properties of metal NPs have been previously investigated by optical spectroscopy, atomic force microscopy (AFM), and transmission electron microscopy (TEM) techniques. Core–shell NPs are very attractive for analytical, biological, biochemical, and biotechnological applications due to their unique properties, especially in tuning of plasmon absorption peak (16, 40, 53, 56, 66, 67). It is also interesting to use core–shell NPs with possible plasmon resonance wavelength in the range of 400–500 nm or in other spectral range. The optical properties of spherical core–shell NPs depend on the values of core and shell radii,

and the optical indexes of refraction and absorption of core and shell metals (16, 53, 56, 66, 67). Extending the Mie theory of radiation, the modeling of optical properties of spherical core-shell particles can be carried out for wavelength in range 300 nm $\leq \lambda \leq$ 650 nm (14). In order to obtain high-efficiency factors of absorption, scattering, and extinction of radiation by the core-shell particles, it was observed that the ideal range of shell thickness and core radii should be 0-40 nm and 5-100 nm, respectively. It could be applied for photonic applications in nanotechnology (72). It is possible to control the absorption in the visible range with relatively narrow absorption for each sample by simply controlling two parameters such as shell thickness and core diameter of the particles (53, 56). The controlled and tunable optical properties of metal structures are highly desired for many applications that rely on light absorption of metal such as SERS sensing, imaging therapy, photo catalysis and SPR (16, 40, 53, 56, 66-71, 73). For example, Haes and coworkers explored the long range distance dependence of localized nanosensors using self-assembled monolayer of 11-mercaptoundecanoic acid and Cu²⁺ ions adsorbed on arrays of noble metal NPs with various shapes, sizes, and compositions of the materials (74). We have also shown the plasmonic detection of Cd²⁺ ions using SERS active core-shell NC (66). In addition, we have also developed highly selective visual monitoring of hazardous fluoride ion in aqueous media using thiobarbituric-capped Au NPs (67) and a new way in nanosensor for sensing Fe³⁺ ions in aqueous media (68). Therefore, we have been interested in Au and Ag NPs because they have the strongest plasmonics interaction with light among all metals (15, 16, 40, 53, 56, 66-68). Hence, this review mainly focuses on Au and Ag NPs with different shapes including nanocubes, nanospheres, tetrahedron and octahedron shapes of the particles, etc., where the shape-controlled chemical syntheses of plasmonics metal NPs have also been emphasized. Some unique properties enabled by the shapecontrolled synthesis of metal NPs and NCs as well as the advantages of these structures to several analytical applications such as molecular detection and determination in different fields have been highlighted in this review. To summarize our discussion, the specific examples of localized surface plasmon resonance (LSPR) sensing experiments using wavelength shift and SERS have been provided. The review ends with a perspective of the field, identifying the main challenges to be overcome and suggesting areas where the most promising developments are likely to happen in future.

Surface plasmon resonance

Metallic nanostructures

The physical origin of the strong light absorption by metal NPs is the coherent oscillation of the conduction band electrons induced by interaction with an electromagnetic radiation. This collective oscillation of conduction electrons in metals is known as plasmon. To explain the formation of dipole and origin of plasmon in metals upon interaction with electromagnetic radiations, metals can be considered as plasma of positive ions having equal numbers of conduction electrons. In neutral case, the negatively charged cloud of electron and the positively charged cloud of ions overlap each other. By some external disturbance, such as interaction with electrons or electromagnetic radiations, the charged cloud is disturbed and the electrons moved away from the equilibrium position. If the density of electrons in one region increases, then they repel each other and tend to return to their original position. Due to repulsion, electrons move toward their original equilibrium position with certain kinetic energy. As such,

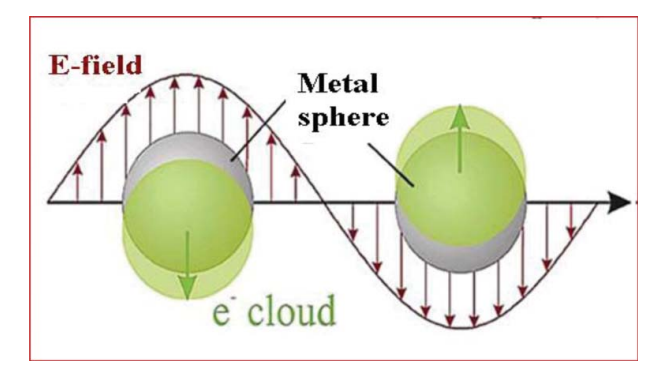


Figure 1. Schematic representation of plasmon oscillations from a sphere that shows the displacement of conduction electron charge cloud relative to the nuclei (shown in light green color). Reprinted with permission from Ref. (77).

they oscillate back and forth. As the net charge difference occurs at the NP's boundaries or surfaces, the electrons on the surface are the most significantly involved in oscillations and their collective oscillations are known as surface plasmon. The resonance between these oscillations and incidence light gives rise to an intense peak in the visible range of the electromagnetic region and is known as SPR (75, 76). The scattering of light by small particles is explained involving the Mie theory and is shown in Figure 1, which shows the displacement of the conduction electron charge cloud relative to the nuclei (14, 77).

Tuning the surface plasmon resonance band of metallic nanostructures

Silver and gold NPs have been studied for their unique optical properties in a wide spectral range. These particles show the SPR band in the visible range of the electromagnetic spectrum. The position of the spectrum depends on various factors such as the size, shape, and dielectric constant of the medium in which they are dispersed (3, 4, 8-10, 77). These SPR bands of metal NPs can be varied by changing their sizes in the range of 1-100 nm (15, 16, 53, 56, 66-68). In contrast, surface plasmon band can be tuned in the region from visible to near infrared by varying some of the above mentioned factors (78). In other words, the position of the SPR bands varied in the visible region with various morphologies and structures of gold and silver NPs is shown in Figure 2A (78). When a transition in shape from sphere to rod is made, a single plasmon absorption band shown in Figure 2B(a) splits into two plasmon bands as shown in Figure 2B(b) (68).

At higher wavelengths, a peak is observed due to longitudinal plasmon resonance along longer axis, while at shorter wavelengths, a peak is observed due to transverse plasmon resonance along shorter axis. Nanorods of gold exhibit two SPR peaks as shown in Figure 2B(b) (68), where the transverse mode and the wavelength of longitudinal mode can be tuned in the spectral region from visible to near infrared depending on their aspect ratio (79). Along with the shape and size of the particles, SPR depends on Rayleigh scattering from NPs (80), charge transfer interactions (81), changes in local refractive index (82), aggregation of NPs (83), etc. These kinds of interactions are very useful in the detection of various analytes including biomolecules using metallic nanostructures. Figure 2A clearly shows that tuning of SPR band over a wide spectral range is possible by making nanostructures of different shapes.

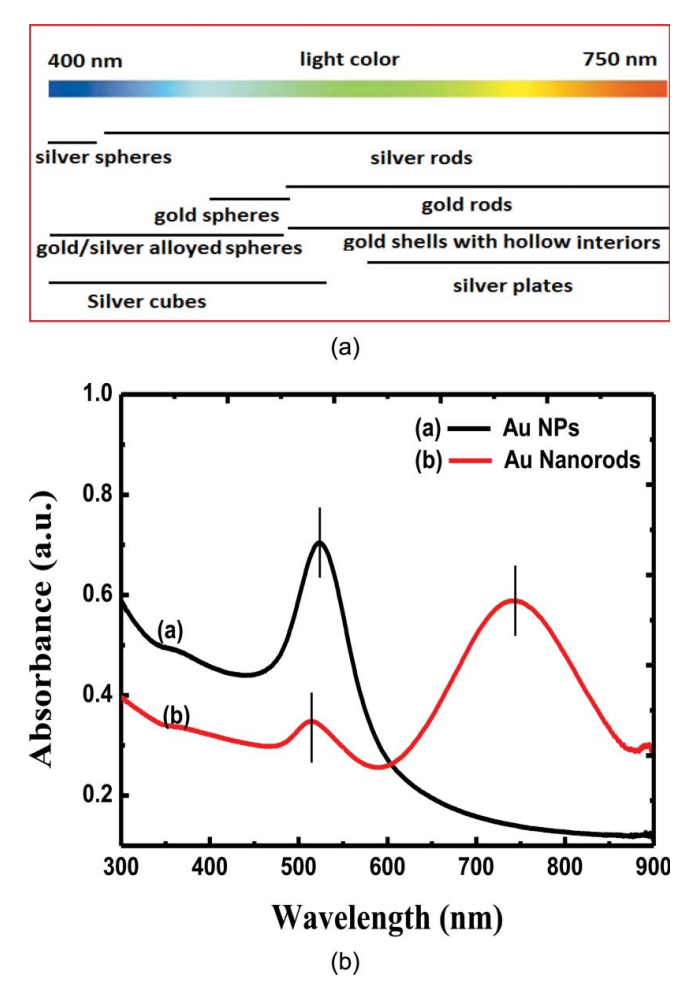


Figure 2. (A) Position of surface plasmon resonance bands tuned using gold and silver nanoparticles of various morphologies and structures. Reprinted with permission from Ref. (78). (B) Surface plasmon resonance spectra of (a) gold nanoparticles and (b) gold nanorods (68).

Localized surface plasmon resonance (LSPR)

The great interest in plasmonic NPs, especially Au and Ag, is enhanced by their fascinating applications in different fields of analytical chemistry (1–3, 15, 16, 19–26, 33–38, 40, 42–44, 49, 50, 52, 55, 65, 73, 80, 83, 84). Additionally, due to the scattering and absorption of light, plasmonic NPs also enhance the electromagnetic fields. For localized surface plasmon, light interacts with particles much smaller than the incident wavelength. The collective oscillation of free electrons is confined to a finite volume as in the case of metal NPs, the corresponding plasmon is called a LSPR. The LSPR can create intense electric field very close to (within a few nanometers) a particle surface resonance. This near field effect can improve SERS cross sections for the molecules adsorbed onto the surface. Thus, the LSPR depends upon the refractive index of the medium surrounding the metal (Au, Ag, Al, and Cu) NPs, which are examined by the electrodynamics approach. However, the localized studies have been focused on Au and Ag NPs for many years because of their bulk dielectric properties (6, 9). The dependence of

refractive index sensitivity and the figure of merit of plasmonic sensors depending on selected metal NPs with similar geometry show that sensing parameters have shape and width below 20 nm (84). The metals (Au, Cu, and Ag) NPs show much higher refractive index sensitivity, but the figure of merit is higher for Ag compared to other metals (85). The observed sensitivity of nanocubes plasmon is shown to be dependent on various parameters such as surface scattering, dynamic depolarization, radiation damping, and interband transition (86).

The first synthesis of plasmonic metal NPs was reported more than 150 years ago when Faraday prepared Au colloids by reducing an aqueous solution of Au chloride with phosphorus (87). A variety of chemical methods have been reported during the past few years for preparing high-quality Au and Ag NPs, which have led to systematic studies of LSPR dependencies on the NPs (9, 10, 53, 56, 84–86). This is because the shape of the NPs can significantly affect the interaction of light and thus LSPR (3, 4, 8, 10, 16, 25, 65).

Metal nanoparticle shape and size dependence on LSPR

The frequency and intensity of plasmon resonance are determined by the intrinsic dielectric properties of the metals, dielectric constant of the medium which it is in contact with and surface polarization. As any variation in shape and size of metallic NPs alters the spectral signature of its plasmon resonance, the ability to change shape and size of the particles and the study of its effect on LSPR are the important and challenging tasks. The interaction of an electromagnetic wave with NPs can be understood by Maxwell's equations (14). Maxwell's equations, based on analytical formulations such as the Mie theory, are desirable for special cases such as solid sphere, concentric spherical shell, infinite cylinder, etc. (14). Numerical calculations with some approximation are required for other particles having arbitrary geometrical shapes. Apart from above-mentioned numerical approaches, the discrete dipole approximation (DDA) has also been used to simulate the interaction of light with metallic NPs having arbitrary shapes (88, 89).

The discrete dipole interaction is used to investigate the effect of shape on LSPR. Dipole approximation calculations are integrated with experimental studies to achieve better understanding of LSPR spectra obtained from NPs' sample (90). These calculations also provide useful guidelines for the design and fabrication of novel plasmonic NPs (90). The LSPR spectra for Ag NPs of various shapes are shown in Figure 3.

The absorption, scattering and extinction spectra for 40 nm silver sphere in water (Figure 3A) and for all the other shapes of the particles were obtained by using the Mie theory (where DDA method was used) (89). The DDA calculated spectra of Ag cube with edge length 40 nm is shown in Figure 3B. In Figure 3B, the absorption spectrum for 40 nm silver spheres shows the presence of two resonance peaks: The main dipole resonance peak is at 410 nm and a smaller quadruple resonance at 370 nm is present as a shoulder peak. The weaker quadruple resonance arising from energy losses make the incident light non-uniform across the sphere and induces a weaker quadruple resonance, characterized by two parallel dipoles of opposite signs (91, 92). Surface polarization is the most important factor in determining the frequency and intensity of plasmon resonance for a given metal NPs because it provides the main restoring force for electron oscillation. Indeed, any variation in particle's shape, size, and the medium will change the surface polarization (93). The nanocubes (Figure 3B) have several distinct symmetries for dipole resonance compared to only one for the sphere (Figure 3A), and hence nanocubes exhibit more peaks than the spheres (94).

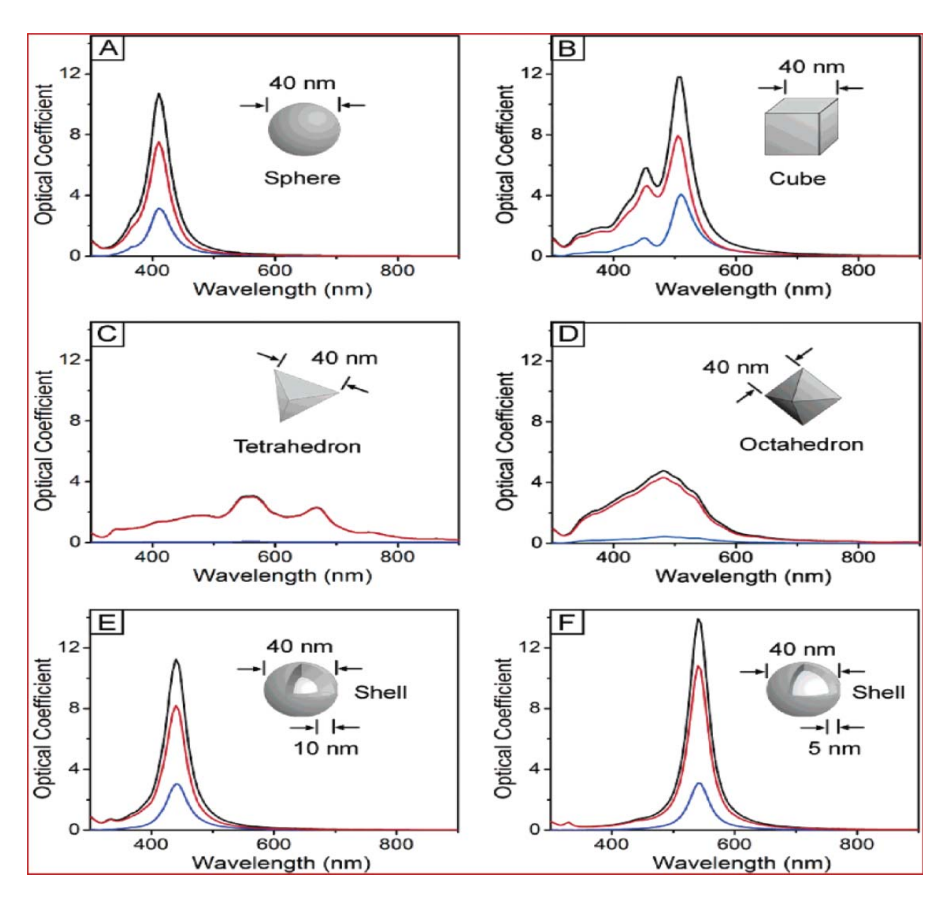


Figure 3. UV–vis extinction (black), absorption (red), and scattering (blue) spectra calculated for silver nanoparticles of different shapes: (A) anisotropic sphere exhibit spectra with a single dipole resonance peak, (B) a cube, (C) a tetrahedron, (D) an octahedron spectra exhibiting multiple red-shifted resonance peaks, (E) hollow sphere peak exhibiting red-shift and (F) thin-shelled wall peak, exhibiting further red-shift. Reprinted with permission from Ref. (94).

Similar trends are observed for the tetrahedron and octahedron, even though they have reduced scattering cross section because of their different symmetries and smaller structures. The simulated spectra of tetrahedron and octahedron (Figure 3C and D) show red-shifted LSPR peaks because they have even sharper corners than the cubes. The tetrahedron shows the red-shifted resonance of three platonic sides because it has the sharpest corners. The calculated hollow spheres or shells also show the red-shifted resonance peak (Figure 3E and F). This shows that the incident electric field induces surface polarization, i.e., surface charges on both; inside and outside of the shell, i.e., hollow spheres. Hence, the particles must have a dipole moment to compensate the incident field. The charges on the inner surface are of the same sign as those on the outer surface for a given pole. The frequency of oscillation is reduced so as to increase the charge separation. For the thin shells, stronger coupling occurs between inside and outside of the shell leading to an increase in charge separation, and the red-shifted spectra is obtained (Figure 3F). Thus, a metallic nanoshell represents a unique object of radiative and local field properties which can be effectively tuned over a wide range (95).

In summary, the DDA calculations show several pathways in which shapes of metallic nanostructure affect the intensity as well as frequency at which the nanostructure scatters and absorbs the light. First, the resonance frequency value depends on the number of ways a nanostructure can be polarized. Second, for nanostructures, the red-shift in the resonance frequency occurs due to the increase in sharpness at the corners, particle anisotropy, and decrease in the wall thickness (in the case of hollow nanostructures). Third, the resonance peak intensity increases with an increase in the symmetry of effective dipole moment of the NPs.

Advantages and limitations of various nanomaterials

Large amount of scientific literature is available on the fabrication techniques of nanomaterials in solution which include photochemical (96–101), electrochemical (102–108), chemical reduction (109–112), ultrasound processing (113–115), sonochemical (116), gamma irradiation, ion irradiation (117–125), microwave processing (126–130), etc. In recent years, the synthetic methods of plasmonics NPs involving different routes have become an important area of research, leading to their direct potential analytical applications (29, 96, 102, 104, 107, 115, 117, 119, 125). We have summarized the advantages and limitations of various synthetic methods and the analytical potential of plasmonics nanomaterials in Table 1. Table 1 also describes the advantages and limitations of various methods for different nanomaterials using object reagents and capping agents and reviews various methods used to obtain the desired shape of Au and Ag NMs (131–156).

Shape-controlled synthesis in plasmonics

In the past two decades, the metallic NPs have evolved for preparing different shapes and sizes of the particles and continuous efforts have been directed toward the shape control synthesis of NPs (3, 4, 8, 75, 77, 86, 94, 106, 116, 124, 128, 130). Wulff's theorem predicts that a single crystal, noble metal NP in an inert gas assumes a truncated octahedron shape at equilibrium (157, 158). In solid-phase synthesis methods, the shapes are different from a Wulff polyhedron due to different anisotropic interactions of different facets with capping agent and solvent. Therefore, the formation of twin structures with energies lower than those of a cuboctahedron occurs. This ascribes that the solution-phase methods of synthesis of plasmonics are more powerful and versatile than vapor-phase methods for the shape-controlled synthesis of noble NPs. Among the various solution-phase methods, polyol reduction is the best established method for generating silver and gold NPs with controlled shape and optical properties (159–164). Herein, we emphasize on the synthesis of metal NPs structures as a model system to fabricate plasmonic NPs with various shapes and LSPR characteristics. Metal NPs can serve as a model system to experimentally probe the effects of quantum confinement on electronics, magnetic, and other related properties.

In the polyol synthesis, the formation of NPs with controlled shapes is facilitated by adding polyvinylpyrrolidone (PVP) as a capping agent. It has been established that the shape taken by PVP in a metallic nanostructure can promote the formation of twin defects included in the initial seed. Different seeds can grow into NPs of different shapes. Figure 4 summarizes all the major shapes that have been observed under different experimental reaction conditions. For example, a single crystal seed can evolve into an octahedron or cuboctahedron or cubes by controlling the relative growth rates along the {100} and {111} directions (164, 165). This type of control is achieved by the introduction of capping agents (166).

Table 1. Different fabrication methods for gold and silver nanomaterials with their advantages and limitations.

Plasmonics nanomaterials	Fabrication method	Capping agent	Reagents/stabilizer	Shapes of particles	Advantages	Limitations	Ref.
Ag@SiO₂ NCs	Chemical reduction Sodium citr	Sodium citrate	Eu-TDPA	Hollow fluorescent nanobubbles	Yield up to 20% enhancement of the fluorescence signal and increase the particle detection sensitivity; used in biological applications such as imaging and sensing	NCs are not in spherical shape	(131)
Au@Ag NCs	Photochemical reduction	Sodium alginate	Sodium alginate and ammonium hydroxide	Colloids	Exact structures of the NPs are not Low yield of gold and silver NPs specified while used photon for reduction	Low yield of gold and silver NPs	(132)
Au@Ag NCs	Radiolysis	NaCN	K[Au(CN) ₂] and NaCN	Spherical	cond, the duration on pulse is much in the heat dissipation eas in the d, pulses are much an this time scale	High yield but not uniform; the laser powers are reported to only absorb rather than absolute energies per pulse	(133)
Ag@SiO ₂ NCs Chemical reduct	Chemical reduction	APTES	Sodium silicate and APTES	Concentric spherical	- e	Bulk data are not reliable; need mathematical method taking into account different attenuation through the core and shell; 10% polydispersity also occurs	(134)
Au@Pd	Sonochemical reduction	SDS	SDS, NaBr and palladium Spherical NPs black	Spherical NPs	Particles are individual monometallic but not bimetallic	EDX data showed NPs are individually monometallic and not bimetallic	(135)
Ag@Au NCs	Reduction	Tyrosine	Tyrosine, octadecylamine Anisotropic Agand NaBH ₄ originating Au NPs capp Au NPs capp multilavers	Anisotropic Ag nanostructures originating from spherical Au NPs capped by multilavers of tvrosine	urs at high pH (pH es are stable for a	Particles are not uniform	(136)
Ag@SiO ₂ NCs	Ag@SiO₂ NCs Sol–gel method	TEOS	TEOS and ammonia	Spherical NCs and plasmonics waveguide structures	Uniform shapes, well-controlled dimensions, multiple wave guiding structures with various geometries can be fabricated in a single step by designing templates at low temperature	The reaction required nearly one hour at room temperature for synthesis	(137)
Au NRs	Seed-mediated growth	CTAB	CTAB and AA	Nanorods		Further increase in pH not only leads to a large proportion of rods but high polydispersity occurs	(138)

(Continued on next page)

Plasmonics nanomaterials	Plasmonics nanomaterials Fabrication method Capping agent	Capping agent	Reagents/stabilizer	Shapes of particles	Advantages	Limitations	Ref.
Au NRs	Combination of chemical reduction and photoirradiation	CTAB	CTAB, AA and TDAB	Nanorods	Using the combination of these two methods, obtained drastic acceleration of the photoreaction and simplification of reaction	The shape can be varied depending on the irradiation time	(139)
Au NPs	Photoirradiation	Extracts itself	Mushroom extract	Less spherical Au NPs	It is effective for anticance property and no lethal effect is observed in vernell lines	Polydispersity occurs	(140)
Au NPs	Biosynthesis	Extracts itself	Terminalia arjuna extract Spherical Au NPs	Spherical Au NPs	сера	None	(141)
Au NPs	Biosynthesis	Extracts itself	Abelmoschus esculentus extract	Spherical NPs with narrow size range of 45–75 nm	Effective antifungal agent; gold NPs are capable of rendering high antifungal efficacy and hence has a great potential in the preparation of drugs used	None	(142)
Au NRs	Seed mediated	CTAB	NaBH ₄ , sodium citrate, AA, and CTAB	Spherical NPs	Particle size can be controlled by varying the seed to metal salt	Yields are very low, addition of small amount of reducing agent inhibits additional nucleation but promotes	(143, 144)
Au NPs	Chemical reduction	SDS	SDS, hydrazine dihydrochloride and	Spherical NPs and NRs	Nucleation enhancement 99% as compared to the particle	Separation of rods and spherical NPs is very difficult	(145)
Au-Ag NPs	Chemical reduction	Oleyamine	Oleylamine, hexane, toluene and 1,2-dichlorohenzene	Spherical NPs	Nearly monodisperse Au and Ag NPs with adjustable sizes and with exchangeable surfactants	Polydispersity occur	(146)
Au NRs	Seed mediated	CTAB	CTAB and AA	Rectangle, hexagon, cube, triangle and starlike	High yield	On increasing the concentration of AA, rod length and yield decreases	(147)

	_
1	∠ '
1.4	-

(148)	(149)	(150)	(151)	(152)	(153)	(154)	(155)	(156)
Single-crystalline and twinned product have similar sizes therefore the separation is not possible	Seeds exhibit limited active lifetimes after which they may introduce time-dependent heterogeneities in resulting size and shape of nanoparticle	Depend on the coating properties and their water uptake on the oxygen content in the coating films and their thickness	Low yield	Majority of polycrystalline nature of particles	Not stable	Polydispersity also occurs	Flat and plate like morphology with polydispersity occuring	At 60 °C, the agglomeration of particles is also influenced by the mixing speed of the reactants, and the speed was slow enough for mixing
High yield and it is more useful than other planar twinned nanoparticles	Seedless approach is used to eliminate chemical reagents; almost identical optical and crystallographic properties up to 90 wt% less reagent material	Homogenous NPs	Nearly spherical and particles are stable for more than 7 years even under ambient conditions	Cluster formation but highly fluorescent Ag NPs are obtained	Unprotected Au NPs are much better catalyst for reduction of HAuCl ₄ using hydroxylamine than the surface-protected nanomaterials	Excellent long-term stability and reproducible uniform modifier films leading to increased reproducible voltametric measurements	Stable Au and Ag NPs are obtained	Stable NPs can be obtained by varying the molar ratio of NaOH and silver nitrate
Au hexagonal bipyramids; twinned Ag triangular nanoprisms	Seedless nanorods and nanoprisms	Plasma polymerized film	Spherical NPs, polyhedron and plate shape	Polycrystalline	Spherical NPs	Thin film of Au NPs on the surface of MWCNTs	Flat and plate nanoparticles	Colloidal nanoparticles
CTAB and AA	NaBH ₄ , AA and CTAB	Ag-Au/polytetrafluoro ethylene NCs and hexamethyldisiloxane	Two polished Ag plates as the anode and cathode and PVP	Cyclohexyl-amine Irgacure 2959, toluene, hexadecylamine, and cyclohexylamine	Benzoins as ketyl precursors, benzophenone, hydroxylamine, tetrahydrofuran, and NaBH ₄	MWCNT, nitric acid and phosphate buffer	Neem leaf broth (Azadirachta indica)	PVP, NaOH, and glucose
ר CTAB	CTAB	PTFE	РΛР	Cyclohexyl-amine	Hydroxyl-amine, tetra- hydrofuran	Open -end MWCNTs with hydrophillic surface	Neem leaf	PVP
Chemical reduction CTAB	Seed mediated	Vapor deposition	Electrochemical	Photochemical	Ag and Au NPs Photochemical	Electrochemical	Biosynthesis	Chemical reduction
Ag NPs	Au NPs	Ag NPs	Ag NPs	Ag NPs	Ag and Au NP	Au NPs	Au @Ag NCs	Ag NPs

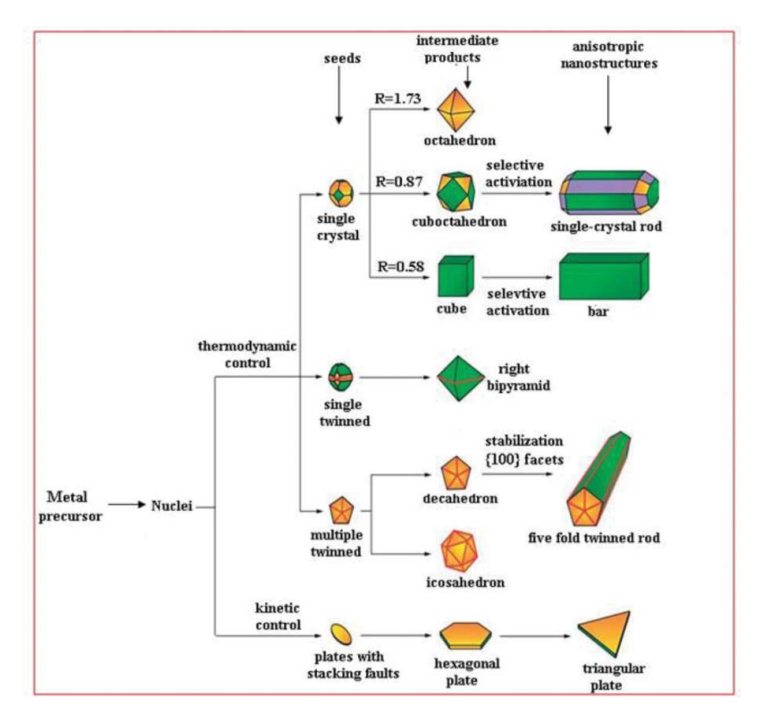


Figure 4. A schematic illustrating the reaction pathways that lead to metal nanoparticles having different shapes. Green, orange, and purple colors represent the $\{100\}$, $\{111\}$, and $\{110\}$ facets, respectively. The parameter R is defined as the ratio of the growth rates along the $\{100\}$ and $\{111\}$ directions, respectively. Reprinted with permission from Ref. $\{173\}$.

Additionally, the single crystal cuboctahedron and cubic seeds can be subjected to anisotropic growth of 1D nanorods into octagonal cross sections and nanobars with rectangular cross sections (165). A single twinned seed can grow into right bipyramids. When the seeds are multiple twinned, they will evolve into decahedrals, icosahedrons, or five-fold twinned rods. Multiple twinned seeds depend the stability of side {100} surface (166–168). Finally, platelike seed can grow into a hexagonal or triangular plate whose top and bottom faces are {111} facets and side surface is enclosed by mix {100} and {111} facets (Figure 4) (169, 170). Figure 4 clearly shows that first a precursor is reduced to form a nuclei. Once the nuclei have grown past a certain size, they become seeds with a single crystal, single twinned, or multiple twinned structure. If shaking faults are introduced, the seeds will grow into plate-like nanostructures.

In summary, in order to prepare plasmonic NPs of the desired shape, it is very difficult to control the internal structures of the seeds. In solution-phase synthesis, small clusters of metal atom can be unstable between single crystal and twinned morphologies under an elevated temperature condition (171). Due to this unstability, the synthesis usually generates a mixture of single crystal and twinned noble metal nanostructures. Thus, in order to form an entirely single crystal structure, twinned seeds must be removed. Seed structures can be controlled in a number of ways such as oxidative etching and kinetic control (172, 173), and thus the effect of oxidative etching on shape-controlled synthesis is discussed in the next section.

Effect of oxidative etching on shape-controlled synthesis

Oxidative etching can be utilized to manipulate the shape and optical properties of NPs. At nanoscale levels, metals tend to nucleate and grow into twinned and multiple twinned particles with their surfaces bounded by the lowest energy {111} facets (174). Using oxidative etching technique, multiple twinned seeds can be removed from the solution, promoting the formation of single crystal NPs. In this approach, the selective etching of twin defects is enabled as its defect sites are more reactive than single crystalline regions. This method has been applied for the preparation of silver nanocubes involving the reduction of AgNO₃ with ethylene glycol in the presence of a capping agent like PVP. Although the shape selectivity mechanism for this process is yet to be fully understood, it is believed that the selective absorption of PVP on various crystallographic planes of silver plays a major role in determining the product morphology. The addition of Cl⁻, Br⁻, and Fe³⁺ to the PVP solution helps toward the generation of nanocubes, bipyramids, and nanowires of silver, respectively. As per a recent study, this oxidative etching mechanism can also be applied to other noble metals like Pt, Pd, Rh, and Ag (164, 175–179).

Figure 5A provides an illustrative summary of single crystal seeds and nanocubes. In the polyol synthesis, after a certain reaction time, ~20 nm spherical single crystal seeds were produced as shown in Figure 5A. Figure 5B and C shows single crystal seeds that were grown into truncated or sharp cubes depending on the kinetics of the reaction. The truncated cubes take more time for surface reconstruction to reduce the surface area and increase the surface of the lowest energy {111} facets at the corners. The normalized extinction spectra of truncated and sharp nanocubes suspended in water are shown in Figure 5D. The main resonance dipole peak for the truncated cubes is located at 440 nm, which is similar to that of a sphere of similar size. The dipole resonance is more pronounced for 90 nm cubes with sharp corners and most intense peaks are red-shifted to 600 nm. This confirms the general trend predicted by DDA calculations that nanostructures with sharp corners display red-shifted extinction peaks and that the number of peaks exhibited by a nanostructures increases with the number of ways in which the electron density can be polarized (179). High yields of the single twinned seeds necessary for the growth of right bipyramids have only been produced in the presence of Br⁻, which may be due to the fact that Br⁻ is less corrossive than Cl⁻. If NaBr is added to the reaction mixture in place of NaCl, then it leads to high yields of single crystal seed. Without the addition of Br or Cl, Ag precursor is reduced quickly to form multiple twinned particles. Thus, Br - enables sufficient etching to eliminate the seeds with multiple twin defects but not so much as to eliminate those seeds with only single twin defect (180). Thus, the concentrations of corrosive anions also play a critical role in controlling the shape of silver NPs during the polyol process (172).

A high-resolution transmission micrograph of single twinned seed in which the {111} facets are obtained from a 15 h reaction sample is shown in Figure 6A. These single twinned seeds grow to form right bipyramids as shown in Figure 6B (75 nm) and in C (150 nm) with their edge lengths increasing with the reaction time. Figure 6D shows normalized extinction spectra for right bipyramids size with edge lengths of 75 nm and 150 nm. The most intense peak shifted from 530 nm to 742 nm with an increase in edge length because of increased charge separation and energy loss related to the large particle. Additionally, bipyramids are significantly sharp where the two halves of the bipyramids meet, leading to a red-shift of the main resonance peak. Such sharp corners improve localized field enhancement for Raman scattering.

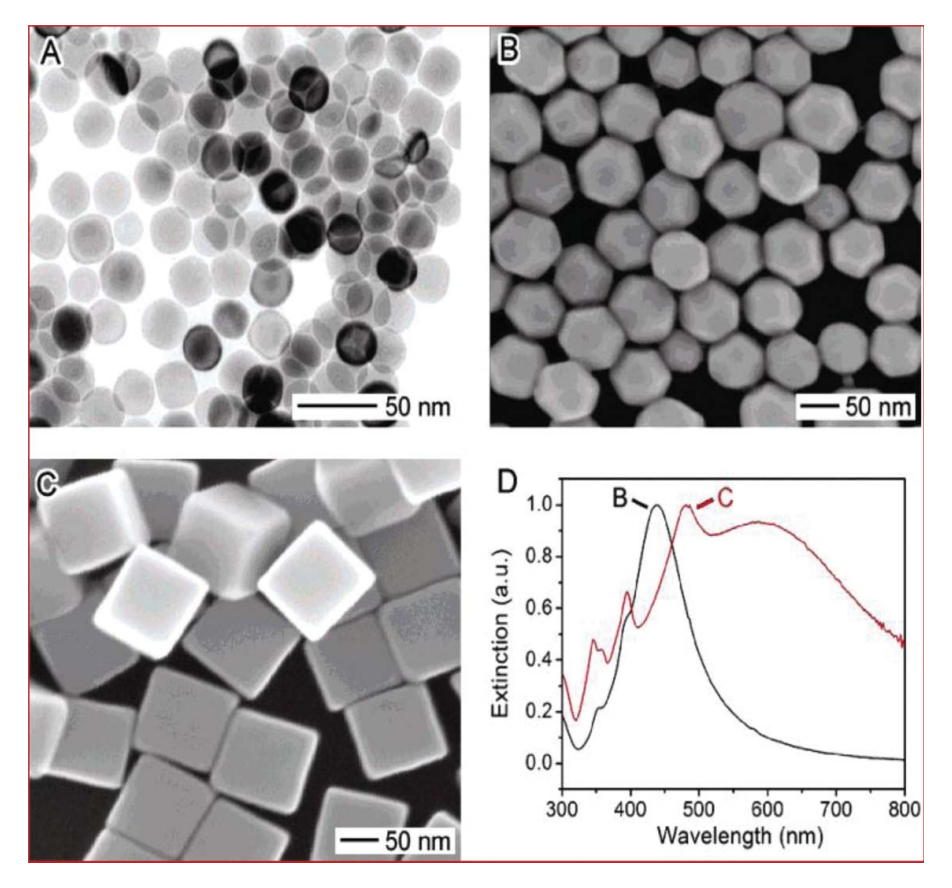


Figure 5. (A) Transmission electron micrograph of single crystal seeds. (B) Scanning electron micrograph of truncated nanocubes. (C) Sharp nanocubes. (D) Localized surface plasmon resonance spectra of aqueous suspensions of silver nanocubes (C) (red-shifted) showing several peaks compared to the spectrum of the truncated cubes (B) resembling more to the LSPR spectrum of nanospheres. Reprinted with permission from Ref. (94).

Triangular plates are also an important class of silver NPs. The sharp corners and edges of triangular plates generate a large electromagnetic field that makes these NPs an interesting candidate for various spectroscopic techniques (181, 182). The growth of triangular plates with controllable sizes and high yields remains a challenge in the synthesis of NPs different shapes and sizes (183–192). This is because the formation of plate-shaped seeds in the solution is not thermodynamically favored. For plate-shaped seeds or other nanostructures, one must achieve kinetic control to slow the reduction in the synthesis of metals or clusters (169, 177, 193, 194). In the case of Au and Ag, it has been suggested that the desired shape can be achieved during the growth of NPs. As crystal growth proceeds, initially these nanoplates achieve a circular cross section, which then evolves into hexagonal and then triangular shapes with an increase in their lateral dimensions (194–197).

Localized surface plasmon resonance (LSPR) sensing

The previous section described the shape-controlled synthesis of metal NPs having different shapes and their impact on LSPR. The development of plasmonic NPs possessing distinct

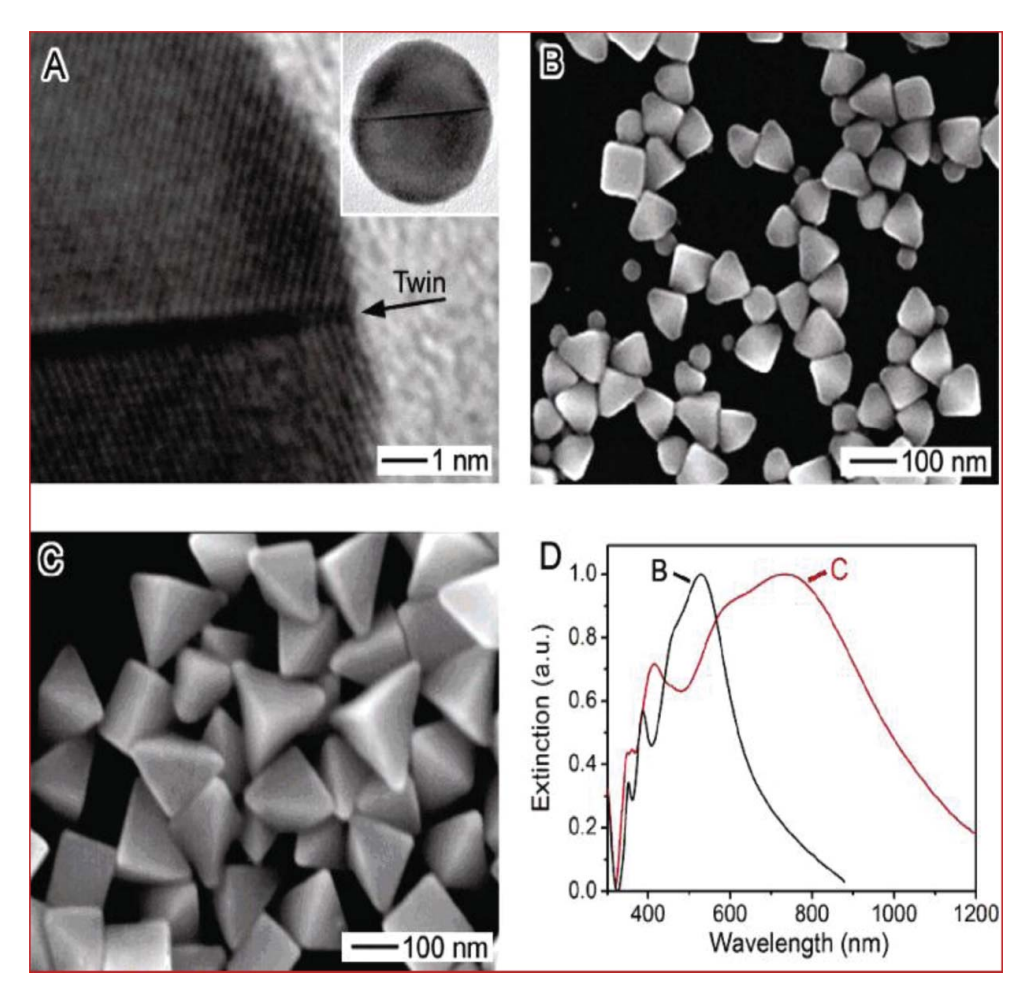


Figure 6. (A) High-resolution transmission micrograph of single twinned seed, which grows to form right bipyramids (B) at 75 nm (C) at 150 nm (D). The localized surface plasmon resonance spectra taken of aqueous suspension of (B) silver nanocubes and (C) silver bipyramids. Reprinted with permission from Ref. (94).

shapes (and hence distinct LSPR spectra) have wide applications such as biological labeling and biomedical applications (198, 199), photothermal therapy (200), LSPR and SERS sensing (201, 202). This section focuses on two different sensing modes like SERS and wavelength shift involving LSPR and their applications to several systems involving the sensing of molecules of biological and chemical interest.

Wavelength shift

The most common method of the LSPR sensing is the wavelength shift measurement wherein the change in the maximum or minimum of the LSPR extinction curve is a function of change in the local dielectric environment caused by the analyte absorption. The sensitivity of the local dielectric environment is correlated to the sensing of biological molecules like proteins and antibodies. Research has been performed for a number of systems in which either the bulk solvent refractive index or the wavelength of a molecular adsorbate is changed, leading to

the detection of biological toxins (203, 204). This principle of local environment has been used to measure the shift in wavelength maxima on binding of either streptavidin or antibiotin to biotin functionalized NPs arrays, i.e., for multiplexed biosensing (205, 206).

In order to systematically study the LSPR response of noble metal NPs to changes in their dielectric environment, a technique is required to produce NPs with desired shape, size, and monodispersity. The chemical synthesis method has been used for this purpose for noble metal nanostructures. These approaches are utilized to fabricate high concentrations of a wide variety of NPs with varying monodispersity and tunable optical properties. The LSPR nanosensors have been useful in detecting metals, biological molecules (9, 36, 43, 74) as well as antigen–antibody reaction (43, 82, 200–202, 204–206). At the nanoscale, the LSPR nanosensor is a refractive index based sensing device that shows the extraordinary optical properties of noble metallic NPs such as Au, Ag, and Cu (36, 74, 82, 205, 207). The LSPR refers to the ability of the conduction electrons in the NPs to oscillate collectively, inducing the electromagnetic field surrounding the NPs, which then determine the sensing volume in which the refractive-based sensing can occur (74, 208). Since the conduction electrons oscillate collectively to only a certain specific wavelength of light, NPs show selective photon absorption, which is easily monitored using ultraviolet–visible spectroscopy (3, 209). Presently, the limit of detection for the LSPR nanosensors has been found to be in the low-picomolar to high-femtomolar region (205).

Silver NPs fabricated from nanosphere lithography technique (NSL), produced consistent red-shift with increase in density and thickness of adsorbate layers (82, 203). NSL is a powerful fabrication technique used to produce arrays of NPs having controlled shape, size, and inter-particle spacing (203, 210). By using NSL, researchers have demonstrated that nanoscale chemosensing and biosensing can be realized through shifts in the LSPR extinction maximum of the tunable silver NPs as shown in Figure 7. This is due to the electromagnetic coupling between NPs. The wavelength shifts are caused by adsorbate induced local

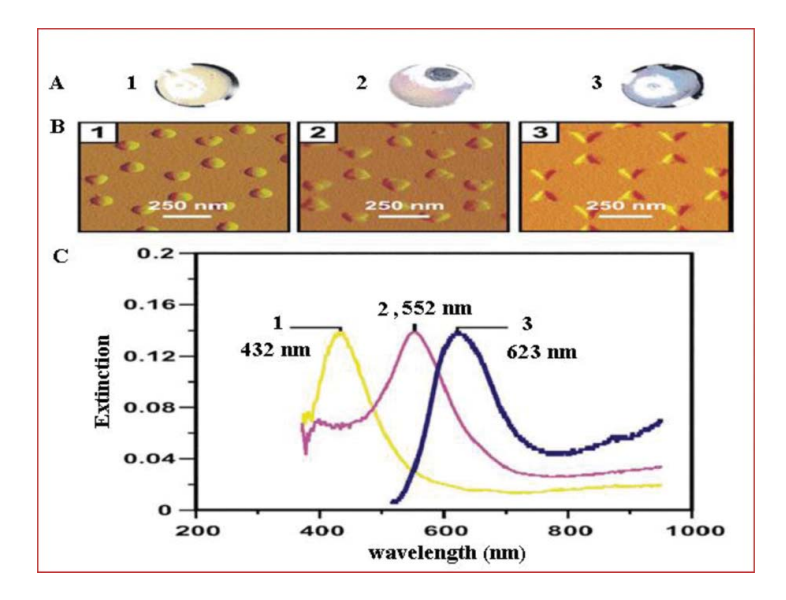


Figure 7. Ag nanoparticle substrate fabricated by NSL. Top row: photographs of nanoparticle substrate. Middle row: AFM images of Ag nanoparticle substrate. Bottom row: normalized UV–vis spectra of nanoparticle substrate. Reprinted with permission from Ref. (212).

refractive index changes in comparison with charge transfer interactions at the surfaces of NPs (211, 212).

Biological sensing has been demonstrated for large proteins and antibodies (43, 213). LSPR has been widely used to monitor a broad range of analyte surface binding interactions including adsorption of small molecules (9, 35, 36, 43, 74, 200–202, 204, 205, 209, 214–216), protein adsorption on self-assembled monolayer (217-219), ligand receptor binding (220-223), antibody-antigen binding (43, 224), protein-DNA interaction (225), and DNA and RNA hybridization (226-229). LSPR sensing has also been demonstrated for sensing of biomarker for Alzheimer's disease in clinical sensing (213, 230) and amyloid-beta derived diffusible ligand (29, 231-233).

Moreover, the LSPR sensing approach can be broadly generalized to allow the diagnosis of any disease with an associated biomarker and antibody pair such as ovarian cancer (234). An alternative approach of LSPR sensing is by attaching chemically synthesized NPs to a substrate using a solid-phase technique. Using this method, chemically synthesized gold and silver NPs are covalently or electrochemically attached randomly to a transparent substrate and could be used for the detection of proteins (234). In this approach, signal transduction depends on changes in the NPs' dielectric environment induced by the solvent or target molecules and not by NPs coupling. Another approach is chip based, and using this method a solvent refractive index sensitivity of 76.4 nm RIU⁻¹ has been found and a detection of 16-nM streptavidin has been achieved (235, 236). This chip-based approach has several merits, including a simple fabrication technique that can be demonstrated in most laboratories as real-time bio-molecules detection using UV-vis spectroscopy and a chip-based design allowing multiplexed analysis. However, the sensitivity of the sensor has been very limited by NPs coupling (235, 236).

Haynes and Van Duyne have investigated the effect of dielectric substrates on the LSPR extinction of metallic arrays (237), while Pinchuk et al. have compared the effects of dielectric, semiconductor, and metallic substrates on NPs (238). It can be concluded from both these investigations that plasmon resonances are red-shifted, which is related to the particles in a vacuum because of interactions as determined by the dielectric constant of the substrate and the distance between the particle and substrate (237, 238). If the particles are in contact with the substrate, then the size of red-shift depends on the particle that is in contact with the substrate (238). Thus, it is important that the enhancement of the substrate's LSPR be properly matched with Raman scattering and excitation wavelength (237–239).

Surface-enhanced Raman scattering (SERS)

Another application for LSPR sensing in which it plays an important role is SERS sensing. Here, we describe the various examples in which SERS is used for applied biological sensing experiments. Raman scattering is a fingerprinting technique for the chemical identification of molecules. Hence, it is used for molecular detection in various fields such as molecular electronics, plasmonic photothermal therapy, single molecule detection, pollutant identification, food minerals, molecular imaging, biomolecules, biowarfare agents, and explosives (16, 25, 26, 35, 40, 50–52, 54, 55, 59, 61, 62, 66–69, 178). As SERS is inherently a weak scattering process, it is necessary to deliberately enhance the scattering signal. To enhance the Raman signal, various improvement methods have been used (15, 16, 40, 53, 56, 66-68). These also include the introduction of intense lasers as photon sources to increase the number of photons for interaction with matter, enhancement of the electric field, and the substrate modification for the reaction to take place. One of the most important applications of nanostructures is SERS. It is based on the enhancement of Raman scattering of an analyte molecule on a roughened metal substrate surface (53, 56, 240-244). However, due to the dependence of the SERS activity on the parameters of the metal substrate structure such as distance from the substrate, orientation, conformation of the molecules, strength of interaction between the molecule and substrate, SERS spectrum differs substantially from normal Raman spectrum for the same molecule in terms of peak intensity distribution and vibrational modes detection (245, 246).

Over the past 15 years, SERS has emerged as a very powerful technique for the detection of ultra-low concentrations of various analytes and single-molecule detection (16, 25, 26, 35, 40, 50-52, 54, 55, 59, 61, 62, 66-69, 178, 247-250). Using SERS technique, one can amplify Raman signals by several orders of magnitude (53, 56). The amplification of signals in SERS is due to the interaction of photons with metals producing large amplifications of the laser field through excitations generally known as plasmon resonance (251). SERS mainly takes place due to chemical and electromagnetic interactions with the analyte molecule/metal surface (252-255). Hence, it is an extremely useful analytical tool for chemical, biochemical, and biomedical sensing. Signal enhancement due to chemical component is because of the interaction between electronic states of molecules and those of the metallic substrate through charge transfer, leading to surface plasmon resonance enhancement with Raman excitation lasers (256). On the other hand, electromagnetic enhancement is a result of the increase in the electric field at sharp points on rough surfaces or regions in the small gaps between NPs or nanostructures (53, 56,). SPR of metallic substrates also helps in the process of signal enhancement. The enhancement of signals depends on selective vibrations as well as overall proximity of the laser excitation wavelength to the SPR wavelength of the substrate. Ag and Au NPs, due to their strong LSPR in the visible range, are good candidates for SERS (15, 16, 40, 53, 56, 66-68). For a given NP, the tunability of SPR to match with the selected laser wavelength leads to the increase in Raman signal.

Raman signal enhancement is also related to other surface enhancement phenomen such as SPR and surface-enhanced fluorescence (257-266). SERS and surface-enhanced fluorescence have regularly been used for quantitative analysis, detection of various analytes and label-free protein detection. Therefore, several research groups have published a lot of progress in this area (16, 25, 26, 35, 50–52, 54, 55, 59, 61, 62, 66–69, 178, 217, 247–250, 261, 264, 265). Further research has to be performed to improve the efficiency of the Raman signal using a variety of new substrates (15, 16, 53, 56) or techniques such as tip enhanced Raman spectroscopy (TERS) (267, 268). However, TERS instrumentation is relatively expensive. This technique is also used for protein detection and structure study (269). The advantage of TERS application is the sensitivity enhancement of U-shape probe (270). A fiber optics Ushape probe-based biosensor of different bending radii has been fabricated by Satija et al., and it was reported that the probe with bending radius around 0.982 mm possesses the maximum sensitivity and used as a point sensor (270). This type of sensors has been used for the detection of glucose in blood and other samples (271, 272). As a point sensor, they require a very less amount of blood sample ($\sim 150~\mu L$) for sensing, which makes them more suitable for commercialization and better than commercial sensors that generally require about 1.5 mL of blood for the detection of glucose. For the measurement of analyte, only the tip of U-shape probe has to be in contact with the sample (271, 272). The response time of proposed sensors is very low and response curves were obtained immediately after immersing the sensing probe in the glucose sample (271-273). These kinds of sensor developments are

still in progress and the device can be commercialized, after optimization of various associated parameters with it for the detection of glucose (271–274).

The assembly of the SERS substrate, which provides enhanced electromagnetic fields, is a must for the glucose monitor, whereby glucose has to approach the metal surface. To develop a glucose sensor for sensing application, researchers have prepared a mixed self-assembled monolayer that has both hydrophilic and hydrophobic components and assembles aluminamodified silver film over nanosphere (FON) substrate. With this functionalized SERS substrate, detection of glucose concentration has been demonstrated using SERS both *in vitro* and *in vivo* (275, 276). The sensor developed by Lyandres et al. provides real-time information on potentially harmful fluctuations in glucose levels (276). SERS also has great potential in high-throughput protein detection (277–289). Several studies have been carried out in recent past to establish SERS active probes applications (277–288). Raman dyes labeled Au NPs have been used to detect proteins and antibodies for immunoassay (277–280). Some SERS probe studies have used fluorescein-labeled antibodies to recognize antigens on metal substrates (290) and also for label-free protein detection (277, 281, 288).

Recently, metal colloids such as Au and Ag NPs and metal NCs have commonly been used as SERS active substrates for biomolecules detection as well as immunoassay (291, 292). A comparative study of SERS emanating from silver-gold core-shell bimetallic NPs and Ag as well as Au NPs for immunoassay concluded that Ag NPs can produce a large SERS effect than Au NPs (293). Other studies have shown that the SERS spectra of proteins on silver films are difficult to reproduce because of protein multi-absorption and aggregation of Ag NPs (294, 295).

Based on strong SERS signal/activity it was concluded that the silica–silver core–shell (SSCS) substrates have a great potential for the investigation of protein–protein, DNA–protein, and DNA–RNA interactions (224–229, 277, 282). The SERS has also been applied in the field of cellular sensing and analysis (296). Generally, NPs are small enough to fit into cells without hindering their normal function. However, there is size limit beyond which they will not be stable inside the cell. If NPs' size is below 20 nm, then the particles might escape out of the cell. If NPs are greater than 80 nm, then they can damage or impede the function of the cell (296). Hence, size factor of the NPs plays a critical role in the SERS study of living cells. The studies by Chithrani and Chan on intercellular SERS research involved imaging at various positions within the cell with resolution greater than $1-\mu m$ (297) where different types of Raman signals were observed, indicating a very complex chemical environment within the cell. It has also been observed by Kneipp et al. that Au NPs tend to aggregate within the cell and become immobile (298). Their study concluded that strong signals from SERS activity were obtained only when cell functioned normally (298).

Recently, in order to improve intercellular sensing and to minimize negative interaction, a small SERS probe using silica-encapsulated hollow Au NPs for immunoassay has been developed by Ko et al. and is proved to perform better than the Au NPs probe (299). The unique structural and optical properties of hollow Au nanospheres provide various benefits like small size, spherical shape, and tunable and smaller absorption from visible to near IR region (291–301). When the size of a material is reduced to the nanoscale, at or below the characteristic length scale that determines their properties, the material acquires completely new properties (302). Recently, Mahmoud et al. have reported the application of hollow and solid metallic NPs in sensing as well as in nanocatalysis and presented a summary of the difference between the solid and hollow NPs in nanocatalysis (302). These authors have also

shown that the observed superior catalytic properties of hollow NPs are due to the catalysis occurring within the cavity of the hollow NPs. The SERS also meets the requirements for a rapid, sensitive, and specific detection technique in the area of food safety (303). The SERSbased approach has been reported for the detection of water-insoluble molecules by applying a hydrophobic surface modification onto the surface of enzymatically generated Ag NPs. Most recently, Jahn et al. have presented a novel SERS-based approach for the detection of illegal water-insoluble molecules, i.e., food dyes, such as Sudan III in presence of riboflavin, as a water-soluble competitor. They have also demonstrated its applicability for the determination of Sudan III in spiked paprika extracts (303).

Surface plasmons exhibit an electromagnetic field that is strongly confined within a metallic interface, which is extremely sensitive to smaller changes in the refractive index associated with the binding of target biomolecules to ligands tethered at the sensor surface (304). Biosensor research has been devoted to various signal transduction methods including optical (304-307), radioactive (308), electrochemical (309-311), bimetallic Au-Ag nanoplate array as a highly active SERS substrate (312), piezoelectric (313, 314), magnetic (315), and mass spectroscopy (316, 317). Signal transduction depends on changes in the NPs' dielectric environment induced by solvent or target molecules. In case of LSPR based sensing, signal transduction also depends on the sensitivity of surface plasmon to inter-particle coupling where the presence of multiple particles in a solution supports localized surface plasmons that are able to interact electrochemically through a dipole coupling mechanism. The broadening and red-shifts of the particles in LSPR can be easily monitored by using UV-vis spectroscopy. Heas and Van Duyne have developed noble metal NPs based LSPR sensors that retain the optical properties of SPR sensors (205).

Tip-enhanced Raman scattering

The TERS is an emerging branch of SERS in which a sharp metallic tip is used (318) where the probe of a scanning tunneling microscope or atomic force microscope is brought in proximity of the analyte to increase their TERS, i.e., Raman signals (318-321). In this technique, the shape of laser-irradiated metallic tip confines optical energy well below the conventional diffraction limit. All nanoscale metallic tips exhibit local field enhancements because of an electrostatic optical lighting rod effect. TERS is useful because of the fact that the detection techniques using far field spectroscopy tool with the sub-wavelength imaging resolution are enabled by plasmonics. Therefore, the combination of Raman chemical fingerprinting and near-field optical imaging has numerous applications in physics, chemistry, biology, and medical sciences (318-327). In addition to its nanoscale resolution, it can extend the capability of SERS in many fields as microdevices in medicine (319). SERS substrate is prepared on to the probe of a scanning probe microscope. The TERS signals can be achieved for analytes that cannot be brought into contact with a metallic substrate. In the TERS, both the sharpness of the tip and smoothness of the surrounding surface are important, leading to a precise control over the intensity and location of the hot spot. However, reproducible and reliable synthesis methods remain a very challenging task. The Raman signal can be monitored as a function of tip-sample distance, which can provide valuable information on the near-field response of the tip (327). Single molecule sensitivity has been developed for TERS (328-333). Using this technique, Zhang et al. have demonstrated improved anthrax biomarker detection (332, 334). The Raman signals of molecules directly below the tip are dramatically enhanced in this technique.



Since the tip radius is only a few tens of nanometers, the lateral resolution reported for TERS is approximately 10-50 nm (318, 319).

Miscellaneous applications of plasmonics

Application of plasmonics in biological field

The SPR has widely been used to measure binding interactions between biomolecules (197, 198, 204-207, 211, 212, 219, 223, 225, 228, 229, 243, 246, 264, 271, 332, 334-336). The SPR absorption is not due to chromophores but due to resonant electron oscillations induced absorption at the metal sample interface when an in-plane wave vector of the incident light matches the wave vector of the surface plasmon. Therefore, the surface plasmon wave vector is observed by the incident free space wave vector and dielectric constant of the metal film (337–340).

It is interesting to note that the SPR angle is very sensitive to the dielectric constant of the metal because the resonance occurs on the metal interface. Therefore, the sensitivity of SPR to biomolecules binding at the surface is due to interactions of evanescent field with the sample (336). Another application of plasmonics in biology is the use of metallic colloids as probes (336). The suspension of metallic colloids shows brilliant colors due to absorption and scattering of light. While the color of particles and surface plasmon absorption band somewhat depend on the size of spherical NPs, they strongly depend on the shape of the NPs (341). For metals such as silver and gold, almost any color or absorption in any part of UV-vis spectrum can be produced by controlling the structures or shape of the NPs. Therefore, various examples on the synthesis of non-spherical nanostructure have been reported in the literature including aggregates, nanorods, nanocages, nanowires, nanospheres, nanoprisms, and nanoplates, and their different plasmon sensing behaviors have been well demonstrated (342–351).

Application of plasmonics in photothermal imaging and therapy

Plasmonic NPs play an important role in various biomedical applications such as imaging and therapy. This technique depends on processes such as antibody-antigen interaction, while the metal nanostructures serve as the light absorber and thermal energy converter. The conjugation of NPs with antibodies complements the properties of the NPs with the selective and specific recognition capability of the antibodies to antigens (352-355). Herein, a few examples of the application of plasmonics in photothermal imaging and therapy are described (352-358) where nanostructures have been conjugated to biological targets such as tissues or cancer cells (355). The metal nanostructures absorb light and convert it into thermal energy and have been used for imaging in vitro and in vivo sample target or for therapeutic treatment like cancer cell destruction or ablation of the sample (357). Jain et al. have reviewed some interesting SPR-enhanced properties of noble metal NPs and their applications to biosystems (353), while Huang et al. have presented a review with special focuss on the involvement of NPs for cancer diagnosis and therapeutics (354).

For the photothermal imaging and therapeutic application, it is desired to match the absorption of the nanostructures with the wavelength of the laser applied. However, as NPs shapes are complex and its size is large for biomedical applications, smaller shape and sized NPs are desired for effective delivery to the locations of interest for the purpose of detection, imaging, etc. In addition, the NPs also can be tuned in the desired manner for photonicsbased imaging and therapy of cancer using SPR (358).



Application of plasmonics in solar cells

Photovoltaics are considered to have the potential to contribute immensely insolving the problem of climate change. In the last few decades, several research groups have studied the application of plasmonics nanostructures towards the reduction of conventional material usage and improvement the efficiency of photovoltaics (359, 360). The plasmonics devices have been utilized to enhance the performance of solar cells through the enhancements of electric field in the absorber and by enhancing the path length of light through the absorber. There has been a great deal of research on thin-film solar cells over the past decades (360, 361). To date, various options of photovoltaics have been reported where surface plasmon polaritons (SPPs) are propagation excitations that arise from the coupling of the light with collective oscillations of the conduction band electrons propagating at the metal-dielectric interface (362, 263). Stuart and Hall pioneered the scattering from NPs, leading to enhanced absorption (364). Several research groups have reported the enhancement of absorption and photocurrent in a variety of solar cell designs involving metal NPs (365-371). The metal NPs act as dipoles and have the advantage that the light striking the metal NPs is scattered into the material with higher permittivity (372, 373). The scattering allows the NPs to act as an anti-reflective coating (374). In an study, Spinelli et al. have confirmed that the NPs arrays of silver placed on top of high refractive index substrates exhibited high transmittance than standard reflection coatings (375). Back et al. and other researchers have confirmed that localized surface plasmons due to metal NPs has been successful in tunable light for solar cells due to which reflection is enhanced (376-378). However, another route to enhance the absorption path length is to couple incident photons to SPPs by nanostructuring the back contact, i.e., reflectors of thin-film solar cells (379-382). Therefore, the localized surface plasmon interaction by imbedded Ag NPs provided substantial and efficient enhancement in solar cells and have been true in the case of other reports (379–382).

Applications of plasmonics in the field of biosensors

Development of sensors is critical to the detection and analysis of various chemicals, toxicants, and biologically important compounds in the areas of clinical, environmental monitoring, security and food safety, etc. Lately, SPR has been applied to the development of biosensors (383-387). The SPR biosensors can detect the interaction of biomolecules without labeling, i.e., they can be used for label-free biomolecules detection. Therefore, SPR biosensors have been used in interaction studies and screening of varieties of moieties like carbohydrates, receptors, proteins, cells, deferent types of bacteria, clinical diagnostics, military defense, etc. (306, 307, 310, 311, 313, 314, 380-382). Due to their salient features like good detection sensitivity, label-free and real-time detection capabilities, SPR-based biosensors have been used in many applications such as detection of bacteria, allergens, pesticides, viruses, etc. For SPR-based biosensors, depending on the size of the target sample, four different types of assay formats such as direct assay, competitive assay, sandwich assay, and inhibition assay have been developed (383).

In the direct assay format, the recognition molecules are immobilized on the surface of the SPR chip. The sample then binds to immobilized recognition element. The direct assay is used for medium and large molecular weight analytes (384). In the competitive assay format, two samples are used: one is free and other is conjugated to larger protein such as

bovine serum albumin competing for the same recognition molecules immobilized on the surface of the SPR sensor. The signal is proportional to the amount of the target sample (385). In the sandwich assay, secondary recognition molecule is captured by an immobilized recognition element by using secondary recognition species to improve the detection range (386). In the inhibition assay format, a conjugate sample is immobilized on a fixed concentration of an antibody and is passed over the SPR surface immobilized sample derivative (387). In the last decade of research, the SPR biosensor technique has received great interest (383–387). Some applications of the SPR biosensors like pesticides, allergens, bacteria, virus, etc. are presented in the following sections.

Plasmonic detection of pesticides

The pesticides analysis is extremely important due to their adverse effect on human health and also due to the the fact that large amounts of pesticides are commonly used. The United States Environmental Protection Agency (USEPA) has recommended the maximum allowable concentrations for most common pesticides like Atrazine and Simazine as 3 $\ \text{ng mL}^{-1}$ and 4 $\ \text{ng mL}^{-1}$, respectively. Therefore, various efforts have been directed to develop sensors for the detection of pesticides at extremely low levels (388-401). A list of pesticides detected using SPR biosensors, showing the sensing materials and techniques used, and the detection limit/range are presented in Table 2.

Table 2. Some examples of pesticides detection using SPR biosensors along with materials and techniques used and the detection limit/range.

Pesticide detected	Sensing materials	Detection limit/range	Instrument/ sensor type	Ref.
Fenamithion and acetamiprid in water	Cd-Te quantum dots with p-sulfonatocalix[4]arene	0.12 nM and 0.34 nM	Luminescence	(388)
Parathion .	Gold electrode	291.26 Da	Quartz crystal microbalance	(389)
Aldrin, dieldrin, chlorpyrifos	Tissue fats and rendering oils	0.005 – $0.1~\mu g~g^{-1}$	Laser induced breakdown spectroscopy	(390)
Organophosphorous	O-ethyl O-4-nitrophenyl phenylphosphonothioate	0.01 μ g mL $^{-1}$	Immuno-chromatographic based sensor	(391)
Carbaryl	Inhibition immunoassay using BSA- CNH conjugate	1.3 $\mu \mathrm{g~mL}^{-1}$	β-SPR	(392)
Atrazine	Competition immunoassay using atrazine-HRP-conjugate	5 ng mL ⁻¹	Biacore-2000	(393)
2,4,5-Trichlorophenoxy acetic acid	Poly-o-toluidine Zr(IV) phosphate nanocomposite	1 μ M	Electrochemical	(394)
Melamine	18-Crown-6 ether functionalized Au NPs	6 ppb	Optical	(395)
Pirimicarb	Molecular imprinted nano-polymers (methacrylic acid with carboxyl functional groups)	$8 \times 10^{-6} \mathrm{M}$	Piezoelectric	(396)
Methyl parathion	Nano-ZrO ₂ /graphite/paraffin	2 ng mL^{-1}	Electrochemical	(397)
Methyl parathion	Fe ₃ O ₄ @Au nanocomposite	0.1 ng mL ⁻¹	Inhibition-based enzyme biosensors	(398)
Chlorphrifos and fenthion	Tangerine juices	$0.20 \pm 0.04 \mu \mathrm{g L^{-1}}$ and 0.50 ± 0.06 $\mu \mathrm{g L^{-1}}$	Immunoassays-based biosensors	(399)
16 pesticides from different chemical groups in water	Polydimethylsiloxane and polyacrylate	$0.015-0.13~\mu \mathrm{g L}^{-1}$	Gas chromatography based sensor	(400)
Paraxon	Indirect immunoassay	1-100 ppb	LSPR	(401)

Table 3. Some examples of bacteria detection using SPR biosensors.

Analyte	Assay format	Detection limit/range	Instrument/ sensor type	Ref.
Listeria monocytogenes	Subtractive inhibition immunoassay	10 ⁵ cfu mL ⁻¹	Biacore-3000	(402)
E.coli O157:H7	Sandwich assay	10^{3} – 10^{7} cfu mL ⁻¹	Optical fiber probes	(403)
E.coli 0157:H7	Sandwich assay	2 cfu mL $^{-1}$ /30 -3×10^4 cfu mL $^{-1}$	SPR biosensor	(404)
E.coli O157:H7	Sandwich assay	10^3 cfu mL $^{-1}$	SPR biosensor	(405)
E.coli O157:H7	Direct immunoassay	$10^{7} \text{ cfu mL}^{-1}/8.7 \times 10^{6}$ cfu mL ⁻¹	Commercially available Spreeta sensor	(406)
Yersinia enterocolitica	Direct immunoassay	10 ² –10 ⁷ cfu mL ⁻¹	Wavelength division multiplexing	(407)
Legionella pneumophila	ELISA immunosorbent assay	$10^8 \mathrm{cfu} \mathrm{mL}^{-1}$	SPR biosensor	(408)
Staphylococcus aureus	Direct immunoassay	10 cfu mL ⁻¹	SPR biosensor	(409)
Campylobacter jejuni	Indirect immunoassay	10^3 cfu mL $^{-1}$	SPR biosensor	(410)
Listeria monocytogenes	Direct immunoassay	10^7 cfu mL $^{-1}$	Biacore-3000	(411)
Vibrio cholerae O1	Direct immunoassay	$3.7 \times 10^{5} \text{ cfu mL}^{-1}$	SPR biosensor	(412)
Acidovorax avenae subsp. citrulli	Direct, subtractive, sandwich immunoassay	$1.6 \times 10^{-6} \text{cfu mL}^{-1}$	SPR biosensor	(413)

Plasmonic detection of bacteria

Generally, the detection of bacteria using SPR biosensors is not an easy task for several reasons. Still, rapid methods for the detection of bacteria are essential, and thus great efforts have been directed to develop methods for their detection in food, industrial, and environmental monitoring, clinical diagnostics and biodefense, food poisoning, water contamination, etc. (402-413). Miyajima et al. have devised a fiber-optic fluoroimmunoassay system with a flow-through cell for rapid on-site determination of E. coli O157:H7 by monitoring fluorescence dynamics (403), while highly sensitive detection of pathogen E. coli O157:H7 by electrochemical impedance spectroscopy was reported by Santos et al. (404). SPR has not only been used for the development of simple biosensors but researchers from the Laboratory for the Analysis of Surfaces of Materials, École Polytechnique de Montreal, Canada have developed a method for the differential detection of methicillin-resistant, methicillin-susceptible, and borderline oxacillin-resistant Staphylococcus aureus by SPR (409). Plasmonic detection has widely been used in environmental pollution remedial management for their unique physicochemical properties, and thus Charlermroj et al. have developed strategies to improve the SPR-based immunodetection of bacterial cells (413). Table 3 provides some examples of bacteria that have been previously detected using SPR biosensors (402-413).

Table 4. Some examples of allergens detection using SPR biosensors alongwith assay format and detection limits.

Analyte detected	Assay format	Detection limit	Sensor type/instrument	Ref.
Shrimp allergen Pen a 1 (tropomyosin)	L-cysteine modified gold electrode	0.15 $\mu \mathrm{g~mL^{-1}}$	Electrochemical	(414)
Cytokine allergen	Label-free immunoassay	19 ng m L^{-1}	Label-free biosensor	(415)
β -Casein	Sandwich assay	85 ng mL^{-1}	Biacore-3000	(416)
Peanut protein	Direct immunoassay	0.7 ng mL^{-1}	SPR biosensor	(417)
Soluble extracts of <i>Lolium</i> perenne pollen	Direct immunoassay	$0.1-1 \mu { m g \ mL}^{-1}$	Biacore	(418)
Histamine	Indirect competitive immunoassay	3 ppb	SPR biosensor	(419)

Table 5. Some examples of virus detection using SPR biosensors along with assay format, i.e., sensing materials used and detection limits.

Types of viruses	Assay format/sensing material	Detecting limit/range	Sensor type/instrument	Ref.
Epstein-Barr	Direct immunoassay	0.2 ng mL ⁻¹	Wavelength division multiplexing based sensor	(420)
Maize chlorotic mottle	Enzyme-based immunosorbent assay	1-1000 ppb	SPR biosensor	(421)
Avian leukosis	Fe ₃ O ₄ @gold quantum dots	115 TCI $D_{50} mL^{-1}$	Immuno-based sensor	(422)
Hepatitis B virus DNA	Au NPs and fluorescein	15 pmol L^{-1}	Fluorescence spectrometer	(423)
Hepatitis B virus DNA	Sandwich immunoassay	50 aM	SERS-based sensor	(424)
Herpes simplex virus type 1	Direct immunosaasy	10 ⁻⁴ fringes	Young interferometer sensor	(425)

Plasmonic detection of allergens

In the last few years, awareness of allergens has led to a growing demand for rapid, reliable, and sensitive devices for identifying and quantifying allergens. Table 4 provides several types of examples of allergens that have been easily detected using SPR biosensors (414–419). The quantification of the major shrimp allergen Pen a 1 (tropomyosin) has successfully been attempted by Jiang et al. using a mast cell-based electrochemical biosensor (414). Muller-Renaud et al. have been successful in quantification of β -casein in milk and cheese using an optical immunosensor (416), while Kobayashi et al. have developed am SPR immunosensor for the detection of histamine based on an indirect competitive immunoreaction (419).

Plasmonic detection of viruses

Viruses rapidly spread in the environment and may cause devastating effects on human health and their social as well as economic development. Therefore, several harmful viruses like Hepatitis B, Avian Leukosis, etc. have been detected in recent years using SPR tools. Table 5 provides some examples of viruses that have been previously detected using SPR biosensors (420–425).

Concluding remarks and future perspectives

Plasmonic NPs play an important role because of their fascinating properties including photothermal imaging, optical, photonics and SERS properties. Both theoretical and experimental calculations have indicated that the plasmonics absorption strongly depends on the structure of the NPs. Any morphological change in plasmonic NPs causes a spectral shift because of the charge separation. The oxidative etching and kinetic control has been utilized to manipulate the shape and optical properties of NPs in the polyol synthesis process that effectively generates NPs of different shapes such as cubes, bars, rods, bipyramids, and triangular and hexagonal plates. In this review, we have emphasized on the shape-controlled synthesis of various NPs and also studied different capping agents and their fascinating analytical applications in different fields.

Finally, the use of LSPR spectroscopy for the biological and chemical synthesis sensing has been discussed using recent reports from the literature. LSPR spectroscopy provides a new direction in analyzing and for further sensing experiments owing to enhanced LSPR shifts. The applications of both wavelength shift and SERS sensing have shown that a variety

of chemically and biologically relevant molecules, like biomarkers of Alzheimer's disease, glucose detection, protein detection, etc., can be easily detected. The plasmonic NPs research continue to grow fast and these LSPR-based sensing experiments will improve as well as lead to high sensitivity, faster and reversible responses, and an ever broadening scope of applicability in different areas of research, especially in analytical and bioanalytical chemistry.

Acknowledgments

The authors are thankful to Professor Aditya Shastri, Vice Chancellor, Banasthali Vidyapith for kindly extending the facilities of "Banasthali Centre for Education and Research in Basic Sciences" sanctioned under CURIE programme of the Department of Science and Technology (DST), Government of India, New Delhi, India. S. Prasad is grateful to the University of the South Pacific for support in various

Funding

J. Boken is thankful to Department of Science and Technology (DST), Government of India, New Delhi, India for financial assistance via grant no. F.No.SR/WOS-A/PS-35/2010.

References

- 1. Liu, C. T., and Tang, A. N. (2015) Applications of nanoparticles in elemental speciation. Anal. Lett. 48: 1031-1043.
- 2. Li, N., Liu, D., and Cui, H. (2014) Metal-nanoparticle-involved chemiluminescence and its applications in bioassays. Anal. Bioanal. Chem. 406: 5561-5571.
- 3. Haynes, C. L., and Van Duyne, R. P. (2001) Nanosphere lithography: A versatile nanofabrication tool for studies of size-dependent nanoparticle optics. J. Phys. Chem. B 105: 5599–5611.
- 4. Tao, A. R., Habas, S., and Yang, P. (2008) Shape control of colloidal metal nanocrystals. Small 4: 310-325.
- 5. (a) Ringe, E., Sharma, B., Henry, A. I., Marks, L. D., and Van Duyne, R. P. (2013) Single nanoparticle plasmonics. Phys. Chem. Chem. Phys. 15: 4110-4129. (b) Jin, R., Cao, Y. C., Hao, E., Metraux, G. S., Schatz, G. C., and Mirkin, C. A. (2003) Controlling anisotropic nanoparticle growth through plasmon excitation. Nature 425: 487-490. (c) Link, S., Wang, Z. L., and El-Sayed, A. M. (1999) Alloy formation of gold-silver nanoparticles and the dependence of the plasmon absorption on their composition. J. Phys. Chem. B 103: 3529-3533.
- 6. Powell, A. W., Wincott, M. B., Watt, A. A. R., Assender, H. E., and Smith, J. M. (2013) Controlling the optical scattering of plasmonic nanoparticles using a thin dielectric layer. J. Appl. Phys. 113: 184311.
- 7. Gonzalez, A. L., Noguez, C., and Barnard, A. S. (2013) Mapping the structural and optical properties of anisotropic gold nanoparticles. J. Mater. Chem. C 1: 3150-3157.
- 8. Ahmad, T., Wani, I. A., Ahmed, J., and Al-Hartomy, O. A. (2014) Effect of gold ion concentration on size and properties of gold nanoparticles in TritonX-100 based inverse microemulsions. Appl. Nanosci. 4: 491-498.
- 9. Murray, W. A., Auguie, B., and Barnes, W. L. (2009) Sensitivity of localized surface plasmon resonances to bulk and local changes in the optical environment. J. Phys. Chem. C 113: 5120-5125.
- 10. Miller, M. M., and Lazarides, A. A. (2005) Sensitivity of metal nanoparticle surface plasmon resonance to the dielectric environment. J. Phys. Chem. B 109: 21556–21565.
- 11. Chen, J., Saeki, F., Wiley, B. J., Cang, H., Cobb, M. J., Li, Z. Y., Au, L., Zhang, H., Kimmey, M. B., Li, X. D., and Xia, Y. (2005) Gold nanocages: Bioconjugation and their potential use as optical imaging contrast agents. Nano Lett. 5: 473-477.



- 12. Sun, Y., Mayers, B., and Xia, Y. (2003) Metal nanostructures with hollow interiors. Adv. Mater. 15: 641-646.
- 13. Loo, C., Lowery, A., Halas, N., West, J., and Drezek, R. (2005) Immunotargeted nanoshells for integrated cancer imaging and therapy. *Nano Lett.* 5: 709–711.
- 14. Hsu, C. W., Delacy, B. G., Johnson, S. G., Joannopoulos, J. D., and Soljacic, M. (2014) Theoretical criteria for scattering dark states in nanostructured particles. Nano Lett. 14: 2783-2788.
- 15. Boken, J., Dalela, S., Sharma, C. K., and Kumar, D. (2013) Detection of pathogenic Escherichia coli (E. coli) using robust silver and gold nanoparticles. J. Chem. Eng. Process Technol. 4: 1000175.
- 16. Thatai, S., Khurana, P., Boken, J., Prasad, S., and Kumar, D. (2014) Nanoparticles and core-shell nanocomposite based new generation water remediation materials and analytical techniques: A review. Microchem. J. 116: 62-76.
- 17. Templeton, A. C., Wuelfing, W. P., and Murray, R. W. (2000) Monolayer-protected cluster molecules. Acc. Chem. Res. 33: 27-36.
- 18. El-Sayed, M. A. (2001) Some interesting properties of metals confined in time and nanometer space of different shapes. Acc. Chem. Res. 34: 257–264.
- 19. Lewis, L. N. (1993) Chemical catalysis by colloids and clusters. Chem. Rev. 93: 2693–2730.
- 20. Tani, T. (2015) Silver nanoparticles: From silver halide photography to plasmonics. Oxford Scholarship Online. DOI:10.1093/acprof:oso/9780198714606.001.0001.
- 21. Pena, S. R. N., Freeman, R. G., Reiss, B. D., He, L., Pena, D. J., Walton, I. D., Cromer, R., Keating, C. D., and Natan, M. J. (2001) Submicrometer metallic barcodes. Science 294: 137-141.
- 22. Maier, S. A., Brongersma, M. L., Kik, P. G., Meltzer, S., Requicha, A. A. G., and Atwater, H. A. (2001) Plasmonics – A route to nanoscale optical devices. Adv. Mater. 13: 1501–1505.
- 23. Kamat, P. V. (2002) Photophysical, photochemical and photocatalytic aspects of metal nanoparticles. Phys. Chem. B 106: 7729-7744.
- 24. Murray, C. B., Sun, S., Doyle, H., and Betley, T. (2001) Monodisperse 3 d transtion-metal (Co, Ni, Fe) nanoparticles and their assembly into nanoparticle superlattices. MRS Bull. 26: 985–991.
- 25. Nie, S., and Emory, S. R. (1997) Probing single molecules and single nanoparticles by surfaceenhanced Raman scattering. Science 275: 1102-1106.
- 26. Dick, L. A., McFarland, A. D., Haynes, C. L., and Van Duyne, R. P. (2002) Metal film over nanosphere (MFON) electrodes for surface-enhanced Raman spectroscopy (SERS): Improvements in surface nanostructure stability and suppression of irreversible loss. J. Phys. Chem. B 106: 853-860.
- 27. Alonso, A., Macanas, J., Shafir, A., Munoz, M., Vallribera, A., Prodius, D., Melnic, S., Turta, C., and Muraviev, D. N. (2010) Donnan-exclusion-driven distribution of catalytic ferromagnetic nanoparticles synthesized in polymeric fibers. Dalton Trans. 39: 2579–2586.
- 28. Gonzalez, A. L., and Noguez, C. (2007) Influence of morphology on the optical properties of metal nanoparticles. Comput. Theor. Nanosci. 4: 231-238.
- 29. Haes, A. J., Chang, L., Klein, W. L., and Van Duyne, R. P. (2005) Detection of a biomarker for Alzheimer's disease from synthetic and clinical samples using a nanoscale optical biosensor. J. Am. Chem. Soc. 127: 2264-2271.
- 30. Dolai, S., Dass, A., and Sardar, R. (2013) Photophysical and redox properties of molecule-like CdSe nanoclusters. *Langmuir* 29: 6187–6193.
- 31. Haes, A. J., Stuart, D. A., Nie, S., and Van Duyne, R. P. (2004) Using solution-phase nanoparticles, surface-confined nanoparticle arrays and single nanoparticles as biological sensing platforms. J. Fluoresc. 14: 355–367.
- 32. Kabashin, A. V., Evans, P., Pastkovsky, S., Hendren, W., Wurtz, G. A., Atkinson, R., Pollard, R., Podolskiy, V. A., and Zayats, A. V. (2009) Plasmonic nanorod metamaterials for biosensing. *Nat. Mater.* 8: 867–871.
- 33. Yonzon, C. R., Jeoung, E., Zou, S., Schatz, G. C., Mrksich, M., and Van Duyne, R. P. (2004) A comparative analysis of localized and propagating surface plasmon resonance sensors: The binding of concanavalin A to a monosaccharide functionalized self-assembled monolayer. J. Am. Chem. Soc. 126: 12669-12676.
- 34. Yonzon, C. R., Stuart, D. A., Zhang, X., McFarland, A. D., Haynes, C. L., and Van Duyne, R. P. (2005) Towards advanced chemical and biological nanosensors - An overview. Talanta 67: 438-448.



- 35. Yonzon, C. R., Zhang, X., and Van Duyne, R. P. (2003) Localized surface plasmon resonance immunoassay and verification using surface-enhanced Raman spectroscopy. Proc. SPIE: Int. Soc. Opt. Eng. 5224: 78-85.
- 36. Malinsky, M. D., Kelly, L., Schatz, G. C., and Van Duyne, R. P. (2001) Chain length dependence and sensing capabilities of the localized surface plasmon resonance of silver nanoparticles chemically modified with alkanethiol self-assembled monolayers. J. Am. Chem. Soc. 123: 1471-1482.
- 37. Jung, L. S., Campbell, C. T., Chinowsky, T. M., Mar, M. N., and Yee, S. S. (1998) Quantitative interpretation of the response of surface plasmon resonance sensors to adsorbed films. Langmuir 14: 5636–5648.
- 38. Smith, E. A., and Corn, R. M. (2003) Surface plasmon resonance imaging as a tool to monitor biomolecular interactions in an array based format. Appl. Spectrosc. 57: 320A-332A.
- 39. Brockman, J. M., Nelson, B. P., and Corn, R. M. (2000) Surface plasmon resonance imaging measurements of ultrathin organic films. Annu. Rev. Phys. Chem. 51: 41-63.
- 40. Thatai, S., Khurana, P., Prasad, S., Soni, S. K., and Kumar, D. (2016) Trace colorimetric detection of Pb²⁺ using plasmonic gold nanoparticles and silica-gold nanocomposites. *Microchem. J.* 124: 104-110.
- 41. Valsecchi, C., and Brolo, A. G. (2013) Periodic metallic nanostructures as plasmonic chemical sensors. Langmuir 29: 5638-5649.
- 42. Endo, T., Kerman, K., Nagatani, N., Takamura, Y., and Tamiya, E. (2005) Label-free detection of peptide nucleic acid-DNA hybridization using localized surface plasmon resonance based optical biosensor. Anal. Chem. 77: 6976-6984.
- 43. Endo, T., Yamamura, S., Nagatani, N., Morita, Y., Takamura, Y., and Tamiya, E. (2005) Localized surface plasmon resonance based optical biosensor using surface modified nanoparticle layer for label-free monitoring of antigen-antibody reaction. Sci. Technol. Adv. Mater. 6: 491-500.
- 44. Englebienne, P. (1998) Use of colloidal gold surface plasmon resonance peak shift to infer affinity constants from the interactions between protein antigens and antibodies specific for single or multiple epitopes. Analyst 123: 1599-1603.
- 45. Raschke, G., Kowarik, S., Franzl, T., Sonnichsen, C., Klar, T. A., and Feldmann, J. (2003) Biomolecular recognition based on single gold nanoparticle light scattering. Nano Lett. 3: 935-938.
- 46. Srituravanich, W., Fang, N., Sun, C., Luo, Q., and Zhang, X. (2004) Plasmonic nanolithography. Nano Lett. 4: 1085-1088.
- 47. Kik, P. G., Maier, S. A., and Atwater, H. A. (2004) Surface plasmons for nanofabrication. *Proc.* SPIE: Int. Soc. Opt. Eng. 5347: 215-223.
- 48. Sundaramurthy, A., Schuck, P. J., Conley, N. R., Fromm, D. P., Kino, G. S., and Moerner, W. E. (2006) Toward nanometer-scale optical photolithography: Utilizing the near-field of bowtie optical nanoantennas. Nano Lett. 6: 355-360.
- 49. Jeanmarie, D. L., and Van Duyne, R. P. (1977) Surface Raman spectroelectrochemistry: Part I. Heterocyclic, aromatic, and aliphatic amines adsorbed on the anodized silver electrode. Electroanal. Chem. 84: 1-20.
- 50. Haynes, C. L., Yonzon, C. R., Zhang, X., and Van Duyne, R. P. (2005) Surface-enhanced Raman sensors: Early history and the development of sensors for quantitative biowarfare agent and glucose detection. Raman Spectrosc. 36: 471-484.
- 51. Mezni, A., Balti, I., Mlayah, A., Jouini, N., and Smiri, L. S. (2013) Hybrid Au-Fe₃O₄ nanoparticles: Plasmonic, surface enhanced Raman scattering, and phase transition properties. Phys. Chem. C 117: 16166-16174.
- 52. Yonzon, C. R., Haynes, C. L., Zhang, X., Walsh, J. T., and Van Duyne, R. P. (2004) A glucose biosensor based on surface-enhanced Raman scattering: Improved partition layer, temporal stability, reversibility, and resistance to serum protein interference. Anal. Chem. 76: 78-85.
- 53. Khurana, P., Thatai, S., Prasad, S., Soni, S., and Kumar, D. (2016) Ag_{core}—Au_{shell} bimetallic nanocomposites: Gold shell thickness dependent study for SERS enhancement. Microchem. J. 124: 819-823.
- 54. Nie, S., and Emory, S. R. (1997) Probing single molecules and single nanoparticles by surfaceenhanced Raman scattering. Science 275: 1102-1106.



- 55. Kneipp, K., Wang, Y., Kneipp, H., Perelman, L. T., Itzkan, I., Dasari, R. R., and Feld, M. S. (1997) Single molecule detection using surface-enhanced Raman scattering (SERS). Phys. Rev. Lett. 78:
- 56. Khurana, P., Thatai, S., Boken, J., Prasad, S., and Kumar, D. (2015) Development of promising surface enhanced Raman scattering substrate: Freckled SiO₂@Au nanocomposites. Microchem. J.
- 57. Pipino, A. C. R., Schatz, G. C., and Van Duyne, R. P. (1994) Surface-enhanced second-harmonic diffraction: Selective enhancement by spatial harmonics. Phys. Rev. B 49: 8320-8330.
- 58. Pipino, A. C. R., Van Duyne, R. P., and Schatz, G. C. (1996) Surface-enhanced second-harmonic diffraction: Experimental investigation of selective enhancement. Phys. Rev. B 53: 4162-4169.
- 59. Yang, W. H., Hulteen, J. C., Schatz, G. C., and Van Duyne, R. P. (1996) A surface-enhanced hyper-Raman and surface-enhanced Raman scattering study of trans-1.2-bis(4-pyridyl) ethylene adsorbed onto silver film over nanosphere electrodes. Vibrational assignments: Experiment and theory. Chem. Phys. 104: 4313-4323.
- 60. Geddes, C. D., Aslan, K., Gryczynski, I., Malicka, J., and Lakowicz, J. R. (2004) Noble metal nanostructures for metal-enhanced fluorescence. Rev. Fluoresc. 1: 365-401.
- 61. Pieczonka, N. P. W., and Aroca, R. F. (2008) Single molecule analysis by surfaced-enhanced Raman scattering. Chem. Soc. Rev. 35: 946-954.
- 62. Golab, J. T., Sprague, J. R., Carron, K. T., Schatz, G. C., and Van Duyne, R. P. (1988) A surface enhanced hyper-Raman scattering study of pyridine adsorbed onto silver: Experiment and theory. Chem. Phys. 88: 7942-7951.
- 63. Jensen, T. R., Van Duyne, R. P., Johnson, S. A., and Maroni, V. A. (2000) Surface-enhanced infrared spectroscopy: A comparison of metal island films with discrete and nondiscrete surface plasmons. Appl. Spectrosc. 54: 371–377.
- 64. Shimizu, K. T., Woo, W. K., Fisher, B. R., Eisler, H. J., and Bawendi, M. G. (2002) Surfaceenhanced emission from single semiconductor nanocrystals. Phys. Rev. Lett. 89: 117401–117404.
- 65. Ghosh, S. K., and Pal, T. (2007) Interparticle coupling effect on the surface plasmon resonance of gold nanoparticles: From theory to applications. Chem. Rev. 107: 4797–4862.
- 66. Thatai, S., Khurana, P., Prasad, S., and Kumar, D. (2015) Plasmonic detection of Cd²⁺ ions using surface-enhanced Raman scattering active core-shell nanocomposite. Talanta 134: 568-575.
- 67. Boken, J., Thatai, S., Khurana, P., Prasad, S., and Kumar, D. (2015) Highly selective visual monitoring of hazardous fluoride ion in aqueous media using thiobarbituric-capped gold nanoparticles. Talanta 132: 278-284.
- 68. Thatai, S., Khurana, P., Prasad, S., and Kumar, D. (2014) A new way in nanosensors: Gold nanorods for sensing of Fe(III) ions in aqueous media. *Microchem. J.* 113: 77–82.
- 69. Huang, X., Jain, P. K., El-Sayed, I. H., and El-Sayed, M. A. (2008) Plasmonic photothermal therapy (PPTT) using gold nanoparticles. Laser Med. Sci. 23: 217-228.
- 70. Huang, X., El-Sayed, I. H., Qian, W., and El-Sayed, M. A. (2006) Cancer cell imaging and photothermal therapy in the near-infrared region by using gold nanorods. J. Am. Chem. Soc. 128: 2115-2120.
- 71. Pustovalov, V. K., Astafyeva, L. G., Galanzha, E., and Zharov, V. P. (2010) Thermo-optical analysis and selection of the properties of absorbing nanoparticles for laser applications in cancer nanotechnology. Cancer Nanotechnol. 1: 35-46.
- 72. Pustovalov, V. K., Astafyeva, L. G., and Fritzsche, W. (2012) Optical properties of core-shell gold-silver and silver-gold nanoparticles for near UV and visible radiation wavelengths. Plasmonics 7: 469-474.
- 73. Zhang, J. Z., and Noguez, C. (2008) Plasmonic Optical properties and applications of metal nanostructures. Plasmonics 3: 127-150.
- 74. Haes, A. J., Zuo, S., Schatz, G. C., and Van Duyne, R. P. (2004) A nanoscale optical biosensor: The long range distance dependence of the localized surface plasmon resonance of noble metal nanoparticles. Phys. Chem. B 108: 109-116.
- 75. Link, S., and El-Sayed, M. A. (2000) Shape and size dependence of radiative, non-radiative and photothermal properties of gold nanocrystals. Int. Rev. Phys. Chem. 19: 409-453.

- 76. Link, S., and El-Sayed, M. A. (2003) Optical properties and ultrafast dynamics of metallic nanocrystals. Ann. Rev. Phys. Chem. 54: 331-366.
- 77. Kelley, K. L., Coronado, E., Zhao, L. L., and Schatz, G. C. (2003) The optical properties of metal nanoparticles: The influence of size, shape, and dielectric environment. Phys. Chem. B 107: 668-677.
- 78. Sun, Y., and Xia, Y. (2003) Gold and silver nanoparticles: A class of chromophores with colors tunable in the range from 400 to 750 nm. Analyst 128: 686–691.
- 79. Nikoobakht, B., and El-Sayed, M. A. (2003) Preparation and growth mechanism of gold nanorods (NRs) using seed-mediated growth method. Chem. Mater. 15: 1957–1962.
- 80. McFarland, A. D., and Van Duyne, R. P. (2003) Single silver nanoparticles as real-time optical sensors with zeptomole sensitivity. Nano Lett. 3: 1057–1062.
- 81. Linnert, T., Mulvany, P., and Henglein, A. (1993) Surface chemistry of colloidal silver: Surface plasmon damping by chemisorbed iodide, hydrosulfide (SH-), and phenylthiolate. Phys. Chem. 97: 679-682.
- 82. Riboh, J. C., Haes, A. J., McFarland, A. D., Ranjit, C., and Van Duyne, R. P. (2003) A nanoscale optical biosensor: Real time immunoassay and nanoparticle adhesion. Phys. Chem. B 107: 1772-1780.
- 83. Thaxton, C. S., Rosi, N. L., and Mirkin, C. A. (2005) Optically and chemically encoded nanoparticle materials for DNA and protein detection. MRS Bull. 30: 376-380.
- 84. Anker, J. N., Hall, W. P., Lyandres, O., Shah, N. C., Zhao, J., and Van Duyne, R. P. (2008) Biosensing with plasmonic nanosensors. Nat. Mater. 7: 442–453.
- 85. Chan, G. H., Zhao, J., Hicks, E. M., Schatz, G. C., and Van Duyne, R. P. (2007) Plasmonic properties of copper nanoparticles fabricated by nanosphere lithography. Nano Lett. 7: 1947–1952.
- 86. Sekhon, J. S., and Verma, S. S. (2012) Rational selection of nanorod plasmons: Material, size, and shape dependence mechanism for optical sensors. *Plasmonics* 7: 453–459.
- 87. Faraday, M. (1857) The bakerian lecture: Experimental relations of gold (and other metals) to light. Phil. Trans. R. Soc. Lond. 147: 145-181.
- 88. Khlebtsov, N. G. (2000) An approximate method for calculating scattering and absorption of light by fractal aggregates. Opt. Spectrosc. 88: 594-601.
- 89. Draine, B. T., and Flatau, P. J. (1994) Discrete-dipole approximation for scattering calculations. Opt. Soc. Am. 11: 1491–1499.
- 90. Lu, X., Rycenga, M., Skrabalak, S. E., Wiley, B., and Xia, Y. (2009) Chemical synthesis of novel plasmonic nanoparticles. Annu. Rev. Phys. Chem. 60: 167–192.
- 91. Fuchs, R. (1975) Theory of the optical properties of ionic crystal cubes. Phys. Rev. B 11: 1732-
- 92. Liu, J. Q., He, M. D., Sun, G. H., Yu, J. M., Chao, X. B., and Wang, L. L. (2013) Plasmon hybridization in trimeric meta-molecules with broken spatial inversion symmetry. Opt. Commun. 294: 325-328.
- 93. Aizpurua, J., Bryant, G. W., Richter, L. J., Garcia de Abajo, F. J., Kelley, B. K., and Mallouk, T. (2005) Optical properties of coupled metallic nanorods for field-enhanced spectroscopy. Phys. Rev. B 71: 235420.
- 94. Wiley, B. J., Im, S. H., Li, Z. Y., McLellan, J., Siekkinen, A., and Xia, Y. (2006) Maneuvering the surface plasmon resonance of silver nanostructures through shape-controlled synthesis. Phys. Chem. B. 110: 15666-15675.
- 95. Teperik, T. V., Popov, V. V., and Garcia de Abajo, F. J. (2004) Radiative decay of plasmons in a metallic nanoshell. Phys. Rev. B 69: 155402.
- 96. Alarcon, E. I., Udekwu, K., Skog, M., Pacioni, N. L., Stamplecoskie, K. G., Gonzalez-Bejar, M., Polisetti, N., Wickham, A., Richter-Dahlfors, A., Griffith, M., and Scaiano, J. C. (2012) The biocompatibility and antibacterial properties of collagen-stabilized, photochemically prepared silver nanoparticles. Biomaterials 33: 4947-4956.
- 97. McGilvray, K. L., Fasciani, C., Bueno-Alejo, C. J., Schwartz-Narbonne, R., and Scaiano, J. C. (2012) Photochemical strategies for the seed-mediated growth of gold and gold-silver nanoparticles. Langmuir 28: 16148-16155.
- 98. Balan, L., Melinte, V., Buruiana, T., Schneider, R., and Vidal, L. (2012) Controlling the morphology of gold nanoparticles synthesized photochemically in a polymer matrix through photonic parameters. Nanotechnology 23: 415705.



- 99. Zhu, X., Wang, B., Shi, F., and Nie, J. (2012) Direct rapid, facile photochemical method for preparing copper nanoparticles and copper patterns. Langmuir 28: 14461-14469.
- 100. Scaiano, J. C., Stamplecoskie, K. G., and Hallett-Tapley, G. L. (2012) Photochemical norrish type I reaction as a tool for metal nanoparticles synthesis: Importance of proton coupled electron transfer. Chem. Commun. 48: 4798-4808.
- 101. Kim, F., Song, J. H., and Yang, P. (2002) Photochemical synthesis of gold nanorods. J. Am. Chem. Soc. 124: 14316-14317.
- 102. Ding, L., Bond, A. M., Zhai, J., and Zhang, J. (2013) Utilization of nanoparticle labels for signal amplification in ultrasensitive electrochemical affinity biosensors: A review. Anal. Chim. Acta 797: 1-12.
- 103. Taleb, A., Yanpeng, X., Munteanu, S., Kanoufi, F., and Dubot, P. (2013) Self-assembled thiolate functionalized gold nanoparticles template toward tailoring the morphology of electrochemically deposited silver nanostructure. Electrochim. Acta 88: 621-631.
- 104. Pruneanu, S., Pogacean, F., Biris, A. R., Coros, M., Watanabe, F., Dervishi, E., and Biris, A. S. (2013) The influence of uric and ascorbic acid on the electrochemical detection of dopamine using graphene-modified electrodes. Electrochim. Acta 89: 246-252.
- 105. Reicha, F. M., Sarhan, A., Abdel-Hamid, M. I., and El-Sherbiny, I. M. (2012) Preparation of silver nanoparticles in the presence of chitosan by electrochemical method. Carbohydr. Polym. 89: 236-244.
- 106. Lai, W., Tang, D., Que, X., Zhuang, J., Fu, L., and Chen, G. (2012) Enzyme-catalyzed silver deposition on irregular-shaped gold nanoparticles for electrochemical immunoassay of alphafetoprotein. Anal. Chim. Acta 755: 62-68.
- 107. Lin, D., Wu, J., Wang, M., Yan, F., and Ju, H. (2012) Triple signal amplification of graphene film, polybead carried gold nanoparticles as tracing tag and silver deposition for ultrasensitive electrochemical immunosensing. Anal. Chem. 84: 3662-3668.
- 108. Gao, F., Zhu, Z., Lei, J., Geng, Y., and Ju, H. (2013) Sub-femtomolar electrochemical detection of DNA using surface circular strand-replacement polymerization and gold nanoparticle catalyzed silver deposition for signal amplification. Biosens. Bioelectron. 39: 199-203.
- 109. Liz-Marzan, L. M. (2013) Gold nanoparticle research before and after the Brust-Schiffrin method. Chem. Commun. 49: 16-18.
- 110. Vijaykumar, M., Priya, K., Nancy, F. T., Noorlidah, A., and Ahmed, A. B. A. (2013) Biosynthesis characterisation and anti-bacterial effect of plant-mediated silver nanoparticles using Artemisia nilagirica. Ind. Crop. Prod. 41: 235-240.
- 111. Johan, M. R., Chong, L. C., and Hamizi, N. A. (2012) Preparation and stabilization of monodisperse colloidal gold by reduction with monosodium glutamate and poly (methyl methacrylate). Int. J. Electrochem. Sci. 7: 4567-4573.
- 112. Ren, X., Tan, E., Lang, X., You, T., Jiang, L., Zhang, H., Yin, P., and Guo, L. (2013) Observing reduction of 4-nitrobenzenthiol on gold nanoparticles insitu using surface enhanced Raman spectroscopy. Phys. Chem. 15: 14196-14201.
- 113. Ledier, A. A., Tremblay, B., and Courty, A. (2013) Synthesis of silver nanoparticles using different silver phosphine precursors: Formation mechanism and size control. Phys. Chem. C 117: 14850-14857.
- 114. Zhang, P., He, J., Ma, X. B., Gong, J. L., and Nie, Z. (2013) Ultrasound assisted interfacial synthesis of gold nanocones. Chem. Commun. 49: 987-989.
- 115. Spadavecchia, J., Barras, A., Lyskawa, J., Woisel, P., Laure, W., Pradier, C. M., Boukherroub, R., and Szunerits, S. (2013) Approach for plasmonic based DNA sensing: Amplification of the wavelength shift and simultaneous detection of the plasmon modes of gold nanostructures. Anal. Chem. 85: 3288-3296.
- 116. Cui, X., Wang, B., Zhong, S., Li, Z., Han, Y., Wang, H., and Moehwald, H. (2013) Preparation of protein microcapsules with narrow size distribution by sonochemical method. Colloid Polym. Sci. 291: 2271-2278.
- 117. Misra, N., Biswal, J., Gupta, A., Sainis, J. K., and Sabharwal, S. (2012) Gamma radiation induced synthesis of gold nanoparticles in aqueous polyvinyl pyrrolidone solution and its application for hydrogen peroxide estimation. Radiat. Phys. Chem. 81: 195-200.



- 118. Hien, N. Q., Phu, D. V., Duy, N. N., and Quoc, L. A. (2012) Radiation synthesis and characterization of hyaluronan capped gold nanoparticles. Carbohydr. Polym. 89: 537-541.
- 119. Biswal, J., Misra, N., Borde, L. C., and Sabharwal, S. (2013) Synthesis of silver nanoparticles in methacrylic acid solution by gamma radiolysis and their application for estimation of dopamine at low concentrations. Radiat. Phys. Chem. 83: 67-73.
- 120. Liu, Y., Chen, S., Zhong, L., and Wu, G. (2009) Preparation of high-stable silver nanoparticle dispersion by using sodium alginate as a stabilizer under gamma radiation. Radiat. Phys. Chem. 78: 251-255.
- 121. Long, D., Wu, G., and Chen, S. (2007) Preparation of oligochitosan stabilized silver nanoparticles by gamma irradiation. Radiat. Phys. Chem. 76: 1126–1131.
- 122. Yamamoto, H., Kazawa, T., Tagawa, S., Naito, M., Marignier, J. L., Mostafavi, M., and Belloni, J. (2013) Radiation-induced synthesis of metal nanoparticles in ethers THF and PGMEA. Radiat. Phys. Chem. 91: 148-155.
- 123. Kumari, M. M., and Philip, D. (2013) Facile one-pot synthesis of gold and silver nanocatalysts using edible coconut oil. Spectrochim. Acta A 111: 154–160.
- 124. Duy, N. N., Du, D. X., Phu, D. V., Quoc, L. A., Du, B. D., and Hien, N. Q. (2013) Synthesis of gold nanoparticles with seed enlargement size by γ -irradiation and investigation of antioxidant activity. Colloids Surf. A 436: 633-638.
- 125. Long, Y., Ran, X., Zhang, L., Guo, Q., Yang, T., Gao, J., Cheng, H., Cheng, T., Shi, C., and Su, Y. (2013) Synthesis of gold nanoparticles with seed enlargement size by γ -irradiation and investigation of antioxidant activity. Mater. Lett. 112: 101-104.
- 126. Du, J., and Xia, Z. (2013) Measurement of the catalytic activity of gold nanoparticles synthesized by a microwave-assisted heating method through time-dependent UV spectra. Anal. Methods 5: 1991-1995.
- 127. Breitwieser, D., Moghaddam, M. M., Spirk, S., Baghbanzadeh, M., Pivec, T., Fasl, H., Ribitsch, V., and Kappe, C. O. (2013) In situ preparation of silver nanocomposites on cellulosic fibers-microwave vs. conventional heating. Carbohydr. Polym. 94: 677-686.
- 128. Fuku, K., Hayashi, R., Takakura, S., Kamegawa, T., Mori, K., and Yamashita, H. (2013) The synthesis of size- and color-controlled silver nanoparticles by using microwave heating and their enhanced catalytic activity by localized surface plasmon resonance. Angew. Chem. Int. Ed. 52: 7446-7450.
- 129. Yanpeng, X., Taleb, A., and Jeqou, P. (2013) Electrodeposition of cobalt films with an oriented fir tree-like morphology with adjustable wetting properties using a self-assembled gold nanoparticle modified HOPG electrode. J. Mater. Chem. A 1: 11580-11588.
- 130. Lohse, S. E., and Murphy, C. J. (2013) The quest for shape control: A history of gold nanorod synthesis. Chem. Mater. 25: 1250-1261.
- 131. Aslan, K., Wu, M., Lakowicz, J. R., and Geddes, C. D. (2007) Fluorescent core-shell Ag@SiO₂ nanocomposites for metal-enhanced fluorescence and single nanoparticle sensing platforms. J. Am. Chem. Soc. 129: 1524-1525.
- 132. Sato, T., Kuroda, S., Takami, A., Yonezawa, Y., and Hada, H. (1991) Photochemical formation of silver-gold (Ag-Au) composite colloids in solutions containing sodium alginate. Appl. Organmet. Chem. 5: 261-268.
- 133. Hodak, J. H., Henglein, A., Giersig, M., and Hartland, G. V. (2000) Coherent excitation of acoustic breathing modes in bimetallic core-shell nanoparticles. Phys. Chem. B 104: 11708–11718.
- 134. Tunc, I., Suzer, S., Correa-Durate, M. A., and Liz-Marzan, L. M. (2005) XPS characterization of Au (Core)/SiO₂ (shell) nanoparticles. *Phys. Chem. B* 109: 7597–7600.
- 135. Mizukoshi, Y., Fujimoto, T., Nagata, Y., Oshima, R., and Maeda, Y. (2000) Characterization and catalytic activity of core-shell structured gold/palladium bimetallic nanoparticles synthesized by the sonochemical method. Phys. Chem. B 104: 6028-6032.
- 136. Selvakannan, P. R., Swami, A., Srisathiyanarayanan, D., Shirude, P. S., Pasricha, R., Mandale, A. B., and Sastry, M. (2004) Synthesis of aqueous Au core-Ag shell nanoparticles using tyrosine as a pH-dependent reducing agent and assembling phase-transferred silver nanoparticles at the airwater interface. Langmuir 20: 7825-7836.



- 137. Lu, Y., Yin, Y., Li, Z. Y., and Xia, Y. (2002) Synthesis and self-assembly of Au@SiO2 core-shell colloids. Nano Lett. 2: 785-788.
- 138. Busbee, B. D., Obare, S. O., and Murphy, C. J. (2003) An improved synthesis of high-aspect-ratio gold nanorods. Adv. Mater. 15: 414-416.
- 139. Niidome, Y., Nishioka, K., Kawasaki, H., and Yamada, S. (2003) Rapid synthesis of gold nanorods by the combination of chemical reduction and photoirradiation processes; morphological changes depending on the growing processes. Chem. Commun. 2376–2377.
- 140. Bhat, R., Sharanbasava, V. G., Deshpande, R., Shetti, U., Sanjeev, G., and Venkataraman, A. (2013) Photo-bio-synthesis of irregular shaped functionalized gold nanoparticles using edible mushroom Pleurotus florida and its anticancer evaluation. J. Photochem. Photobiol. B 125: 63-
- 141. Gopinath, K., Venkatesh, K. S., Ilangovan, R., Sankaranaryana, K., and Arumugam, A. (2013) Green synthesis of gold nanoparticles from leaf extract of Terminalia arjuna, for the enhanced mitotic cell division and pollen germination activity. Ind. Crop. Prod. 50: 737-742.
- 142. Jayaseelan, C., Ramkumar, R., Rahuman, A. A., and Perumal, P. (2013) Green synthesis of gold nanoparticles using seed aqueous extract of Abelmoschus esculentus and its antifungal activity. Ind. Crop. Prod. 45: 423-429.
- 143. Jana, N. R., Gearheart, L., and Murphy, C. J. (2001) Wet chemical synthesis of high aspect ratio cylindrical gold nanorods. Phys. Chem. B 105: 4065-4067.
- 144. Kimling, J., Maier, M., Okenve, B., Kotaidis, V., Ballot, H., and Plech, A. (2006) Turkevich method for gold nanoparticle synthesis revisited. Phys. Chem. B 110: 15700–15707.
- 145. Jana, N. R., Gearheart, L., and Murphy, C. J. (2001) Seeding growth for size control of 5-40 nm diameter gold nanoparticles. Chem. Mater. 13: 2313-2322.
- 146. Hiramatsu, H., and Osterloh, F. E. (2004) A simple large-scale synthesis of nearly monodisperse gold and silver nanoparticles with adjustable sizes and with exchangeable surfactants. Chem. Mater. 16: 2509-2511.
- 147. Sau, T. K., and Murphy, C. J. (2004) Room temperature, high-yield synthesis of multiple shapes of gold nanoparticles in aqueous solution. J. Am. Chem. Soc. 126: 8648-8649.
- 148. Personick, M. L., Langille, M. R., Wu, J. S., and Mirkin, C. A. (2013) Synthesis of gold hexagonal bipyramids directed by planar-twinned silver triangular nanoprisms. J. Am. Chem. Soc. 135: 3800–3803.
- 149. Straney, P. J., Andolina, C. M., and Millstone, J. E. (2013) Seedless initiation as an efficient, sustainable route to anisotropic gold nanoparticles. Langmuir 29: 4396-4403.
- 150. Alissawi, N., Zaporojtchenko, V., Strunskus, T., Kocabas, I., Chakravadhanula, V. S. K., Kienle, L., Schonberg, D. G., and Faupel, F. (2013) Effect of gold alloying on stability of silver nanoparticles and control of silver ion release from vapor-deposited Ag-Au/polytetrafluoroethylene nanocomposites. Gold Bull. 46: 3-11.
- 151. Khaydarov, R. A., Khaydarov, R. R., Gapurova, O., Estrin, Y., and Scheper, T. (2009) Electrochemical method for the synthesis of silver nanoparticles. Nanopart. Res. 11: 1193–1200.
- 152. Maretti, L., Billone, P. S., Liu, Y., and Scaiano, J. C. (2009) Facile Photochemical synthesis and characterization of highly fluorescent silver nanoparticles. J. Am. Chem. Soc. 131: 13972-13980.
- 153. Scaiano, J. C., Billone, P., Gonzalez, C. M., Maretti, L., Marin, M. L., McGilvray, K. L., and Yuan, N. (2009) Photochemical routes to silver and gold nanoparticles. Pure Appl. Chem. 81: 635-647.
- 154. Song, Y. Z., Li, X., Song, Y., Cheng, Z. P., Zhong, H., Xu, J. M., Lu, J. S., Wei, C. G., Zhu, A. F., Wu, F. Y., and Xu, J. (2013) Electrochemical synthesis of gold nanoparticles on the surface of multi-walled carbon nanotubes with glassy carbon electrode and their application. Russ. Phys. Chem. A 87: 74-79.
- 155. Shankar, S. S., Rai, A., Ahmad, A., and Sastry, M. (2004) Rapid synthesis of Au, Ag and bimetallic Au core-Ag shell nanoparticles using Neem (Azadirachta indica) leaf broth. J. Colloid Interface Sci. 275: 496-502.
- 156. Wang, H., Qiao, X., Chen, J., and Ding, S. (2005) Preparation of silver nanoparticles by chemical reduction method. Colloids Surf. A 256: 111-115.
- 157. Wulff, G. (1901) Velocity of growth and dissolution of crystal faces. Z. Kristallogr. 34: 449-530.
- 158. Marks, L. D. (1994) Experimental studies of small particle structures. Rep. Prog. Phys. 57: 603-649.

- 159. Komarneni, S., Li, D. S., Newalkar, B., Katsuki, H., and Bhalla, A. S. (2002) Microwave-polyol process for Pt and Ag nanoparticles. Langmuir 18: 5959-5962.
- 160. Sun, Y., and Xia, Y. (2002) Large-scale synthesis of uniform silver nanowires through a soft, selfseeding, polyol process. Adv. Mater. 14: 833–837.
- 161. Wiley, B., Herricks, T., Sun, Y., and Xia, Y. (2004) Polyol synthesis of silver nanoparticles: Use of chloride and oxygen to promote the formation of single-crystal, truncated cubes and tetrahedrons. Nano Lett. 4: 1733-1739.
- 162. Wiley, B., Sun, Y., Mayers, B., and Xia, Y. (2005) Shape-controlled synthesis of metal nanostructures: The case of silver. Chem. Eur. J. 11: 454-463.
- 163. Feldmann, C. (2003) Polyol-mediated synthesis of nanoscale functional materials. Adv. Funct. Mater. 13: 101-107.
- 164. Xiong, Y., Chen, J., Wiley, B., Xia, Y., Aloni, S., and Yin, Y. (2005) Understanding the role of oxidative etching in the polyol synthesis of Pd nanoparticles with uniform shape and size. J. Am. Chem. Soc. 127: 7332-7333.
- 165. Xiong, Y., Cai, H., Wiley, B. J., Wang, J., Kim, M., and Xia, Y. (2007) Synthesis and mechanistic study of palladium nanobars and nanorods. J. Am. Chem. Soc. 129: 3665-3675.
- 166. Wang, Z. L. (2000) Transmission electron microscopy of shape-controlled nanocrystals and their assemblies. Phys. Chem. B 104: 1153-1175.
- 167. Xiong, Y., McLellan, J. M., Yin, Y., and Xia, Y. (2007) Synthesis of palladium icosahedra with a twinned structure by blocking oxidative etching with citric acid or citrate ion. Angew. Chem. Int. Ed. 46: 790-794.
- 168. Xiong, Y., Cai, H., Yin, Y., and Xia, Y. (2007) Synthesis and characterization of fivefold twinned nanorods and right bipyramids of palladium. Chem. Phys. Lett. 440: 273–278.
- 169. Xiong, Y., McLellan, J. M., Chen, J., Yin, Y., Li, Z. Y., and Xia, Y. (2005) Kinetically controlled synthesis of triangular and hexagonal nanoplates of Pd and their SPR/SERS properties. J. Am. Chem. Soc. 127: 17118-17127.
- 170. Xiong, Y., Washio, I., Chen, J., Cai, H., Li, Z. Y., and Xia, Y. (2006) Poly(vinylpyrrolidone): A dual functional reductant and stabilizer for the facile synthesis of metal nanoplates in aqueous solutions. Langmuir 22: 8563-8570.
- 171. Smith, D. J., Petford-Long, A. K., Wallenberg, L. R., and Bovin, J. O. (1986) Dynamic atomiclevel rearrangements in small gold particles. Science 233: 872–875.
- 172. Wiley, B., Sun, Y., and Xia, Y. (2007) Synthesis of silver nanostructures with controlled shapes and properties. Acc. Chem. Res. 40: 1067-1076.
- 173. Xiong, Y., and Xia, Y. (2007) Shape-controlled synthesis of metal nanostructures: The case of palladium. *Adv. Matter.* 19: 3385–3391.
- 174. Allpress, J. G., and Sanders, J. V. (1967) The structure and orientation of crystals in deposits of metals on mica. Surf. Sci. 7: 1-25.
- 175. Doria, G., Conde, J., Veigas, B., Giestas, L., Almeida, C., Assuncao, M., Rosa, J., and Baptista, P. V. (2012) Noble metal nanoparticles for biosensing applications. Sensors 12: 1657–1687.
- 176. Xiong, Y., Chen, J., Wiley, B., Xia, Y., Yin, Y., and Li, Z. Y. (2005) Size-dependence of surface plasmon resonance and oxidation for Pd nanocubes synthesized via a seed etching process. Nano Lett. 5: 1237-1242.
- 177. Chen, J., Herricks, T., and Xia, Y. (2005) Polyol Synthesis of platinum nanostructures: Control of morphology through the manipulation of reduction kinetics. Angew. Chem. Int. Ed. 44: 2589–2592.
- 178. Zettsu, N., McLellan, J. M., Wiley, B., Yin, Y., Li, Z. Y., and Xia, Y. (2006) Synthesis stability, and surface plasmonic properties of rhodium multipods, and their use as substrates for surfaceenhanced Raman scattering. Angew. Chem. Int. Ed. 45: 1288–1292.
- 179. Cobley, C. M., Skrabalak, S. E., Campbell, D. J., and Xia, Y. (2009) Shape-controlled synthesis of silver nanoparticles for plasmonic and sensing applications. *Plasmonics* 4: 171–179.
- 180. Wiley, B. J., Xiong, Y., Li, Z. Y., Yin, Y., and Xia, Y. (2006) Right bipyramids of silver: A new shape derived from single twinned seeds. Nano Lett. 6: 765-768.
- 181. Yang, W. H., Schatz, G. C., and Van Duyne, R. P. (1995) Discrete dipole approximation for calculating extinction and Raman intensities for small particles with arbitrary shapes. Chem. Phys. 103: 869-875.



- 182. Sajanlal, P. R., Subramaniam, C., Sasanpour, P., Rashidian, B., and Pardeep, T. (2010) Electric field enhancement and concomitant Raman spectral effects at the edges of a nanometer-thin gold mesotriangle. Mater. Chem. 20: 2108-2113.
- 183. Pastoriza, I. S., and Liz-Marzan, L. M. (2002) Synthesis of silver nanoprisms in DMF. Nano Lett. 2: 903-905.
- 184. Chen, S. H., and Carroll, D. L. (2002) Synthesis and characterization of truncated triangular silver nanoplates. Nano Lett. 2: 1003-1007.
- 185. Chen, S. H., Fan, Z. Y., and Carroll, D. L. (2002) Silver nanodisks: Synthesis, characterization, and self-assembly. Phys. Chem. B 106: 10777-10781.
- 186. Yener, D. O., Sindel, J., Randall, C. A., and Adair, J. H. (2002) Synthesis of nanosized silver platelets in octylamine-water bilayer systems. Langmuir 18: 8692-8699.
- 187. Maillard, M., Giorgio, S., and Pileni, M. P. (2002) Silver nanodisks. Adv. Mater. 14: 1084–1086.
- 188. Sun, Y., Mayers, B., and Xia, Y. (2003) Transformation of silver nanospheres into nanobelts and triangular nanoplates through a thermal process. Nano Lett. 3: 675-679.
- 189. Xia, Y., Xia, X., Wang, Y., and Xie, S. (2013) Shape-controlled synthesis of metal nanocrystals. MRS Bull. 38: 335-344.
- 190. Khurshid, H., Li, W., Chandra, S., Phan, M. H., Hadjipanayis, G. C., Mukherjee, P., and Srikanth, H. (2013) Mechanism and controlled growth of shape and size variant core/shell FeO/Fe₃O₄ nanoparticles. Nanoscale 5: 7942-7952.
- 191. Jin, R., Cao, Y., Mirkin, C. A., Kelly, K. L., Schatz, G. C., and Zheng, J. G. (2001) Photoinduced conversion of silver nanospheres to nanoprisms. Science 294: 1901–1903.
- 192. Lim, B., Jiang, M., Tao, J., Camargo, P. H. C., Zhu, Y., and Xia, Y. (2009) Shape-controlled synthesis of Pd nanocrystals in aqueous solutions. Adv. Funct. Mater. 19: 189-200.
- 193. Germain, V., Li, J., Ingert, D., Wang, Z. L., and Pileni, M. P. (2003) Stacking faults in formation of silver nanodisks. Phys. Chem. B 107: 8717-8720.
- 194. Washio, I., Xiong, Y., Yin, Y., and Xia, Y. (2006) Reduction by the end groups of poly(vinyl pyrrolidone): A new and versatile route to the kinetically controlled synthesis of Ag triangular nanoplates. Adv. Mater. 18: 1745-1749.
- 195. Chen, J., Lim, B., Lee, E. P., and Xia, Y. (2009) Shape-controlled synthesis of platinum nanocrystals for catalytic and electrocatalytic applications. Nano Today 4: 81–95.
- 196. Sun, Y., and Xia, Y. (2003) Triangular nanoplates of silver: Synthesis, characterization, and use as sacrificial templates for generating triangular nanorings of gold. Adv. Mater. 15: 695-699.
- 197. Liao, H., Nehl, C. L., and Hafner, J. H. (2006) Biomedical applications of plasmon resonant metal nanoparticles. Nanomedicine 1: 201-208.
- 198. Hu, M., Chen, J. Y., Li, Z. Y., Au, L., Hartland, G. V., Li, X. D., Marquez, M., and Xia, Y. N. (2006) Gold nanostructures: Engineering their plasmonic properties for biomedical applications. Chem. Soc. Rev. 35: 1084-1094.
- 199. Xia, Y., and Halas, N. J. (2005) Shape-controlled synthesis and surface plasmonic properties of metallic nanostructures. MRS Bull. 30: 338-348.
- 200. Xiong, C., and Ling, L. (2013) Localized surface plasmon resonance light-scattering sensor for mercury(II) ion with label-free gold nanoparticles. Nanosci. Nanotechnol. 13: 1406-1410.
- 201. Willets, K. A., and Van Duyne, R. P. (2007) Localized surface plasmon resonance spectroscopy and sensing. Ann. Rev. Phys. Chem. 58: 267-297.
- 202. Sherry, L. J., Chang, S. H., Schatz, G. C., Van Duyne, R. P., Wiley, B. J., and Xia, Y. (2005) Localized surface plasmon resonance spectroscopy of single silver nanocubes. Nano Lett. 5: 2034-
- 203. Hicks, E. M., Zhang, X., Zou, S., Lyandres, O., Spears, K. G., Schatz, G. C., and Van Duyne, R. P. (2005) Plasmonic properties of film over nanowell surface fabricated by nanosphere lithography. Phys. Chem. B 109: 22351-22358.
- 204. Nagatsuka, T., Uzawa, H., Sato, K., Kondo, S., Izumi, M., Yokoyama, K., Ohsawa, I., Seto, Y., Neri, P., Mori, H., Nishida, Y., Saito, M., and Tamiya, E. (2013) Localized surface plasmon resonance detection of biological toxins using cell surface oligosaccharides on glyco chips. Appl. Mater. Interfaces 5: 4173-4180.

- 205. Haes, A. J., and Van Duyne, R. P. (2002) A nanoscale optical biosensor: Sensitivity and selectivity of an approach based on the localized surface plasmon resonance spectroscopy of triangular silver nanoparticles. J. Am. Chem. Soc. 124: 10596–10604.
- 206. Ruemmele, J. A., Hall, W. P., Ruvuna, L. K., and Van Duyne, R. P. (2013) A localized surface plasmon resonance imaging instrument for multiplexed biosensing. Anal. Chem. 85: 4560-4566.
- 207. Haes, A. J., and Van Duyne, R. P. (2003) Nanosensors enable portable detectors for environmental and medical applications. Laser Focus World 39: 153-156.
- 208. Jensen, T. R., Kelly, K. L., Lazarides, A. A., and Schatz, G. C. (1999) Electrodynamics of noble metal nanoparticles and nanoparticle clusters. J. Clust. Sci. 10: 295–317.
- 209. Jensen, T. R., Malinsky, M. D., Haynes, C. L., and Van Duyne, R. P. (2000) Nanosphere lithography: Tunable localized surface plasmon resonance spectra of silver nanoparticles. Phys. Chem. B 104: 10549-10556.
- 210. Hulteen, J. C., and Van Duyne, R. P. (1995) Nanosphere lithography: A materials general fabrication process for periodic particle array surfaces. Vac. Sci. Technol. A 13: 1553-1558.
- 211. Haes, A. J., and Van Duyne, R. P. (2004) Preliminary studies and potential applications of localized surface plasmon resonance spectroscopy in medical diagnostics. Expert Rev. Mol. Diagn. 4: 527-537.
- 212. Haes, A. J., and Van Duyne, R. P. (2004) A unified view of propagating and localized surface plasmon resonance biosensors. Anal. Bioanal. Chem. 379: 920-930.
- 213. Haes, A. J., Hall, W. P., Chang, L., Klein, W. L., and Van Duyne, R. P. (2004) A localized surface plasmon resonance biosensor: First steps toward an assay for Alzheimer's disease. Nano Lett. 4: 1029-1034.
- 214. Sepulveda, B., Angelome, P. C., Lechuga, L. M., and Liz-Marzan, L. M. (2009) LSPR-based nanobiosensors. Nano Today 4: 244-251.
- 215. Jung, L. S., and Campbell, C. T. (2000) Sticking probabilities in adsorption of alkanethiols from liquid ethanol solution onto gold. Phys. Chem. B 104: 11168-11178.
- 216. Jung, L. S., and Campbell, C. T. (2000) Sticking probabilities in adsorption from liquid solutions: Alkylthiols on gold. Phys. Rev. Lett. 84: 5164-5167.
- 217. Frey, B. L., Jordan, C. E., Kornguth, S., and Corn, R. M. (1995) Control of the specific adsorption of proteins onto gold surfaces with poly(L-lysine) monolayers. Anal. Chem. 67: 4452-4457.
- 218. Mrksick, M., Grunwell, J. R., and Whitesides, G. M. (1995) Biospecific adsorption of carbonic anhydrase to self-assembled monolayers of alkanethiolates that present benzenesulfonamide groups on gold. J. Am. Chem. Soc. 117: 12009–12010.
- 219. Rao, J., Yan, L., Xu, B., and Whitesides, G. M. (1999) Using surface plasmon resonance to study the binding of vancomycin and its dimer to self-assembled monolayers presenting d-Ala-d-Ala. J. Am. Chem. Soc. 121: 2629-2630.
- 220. Jung, L. S., Nelson, K. E., Stayton, P. S., and Campbell, C. T. (2000) Binding and dissociation kinetics of wild-type and mutant streptavidins on mixed biotin-containing alkylthiolate monolayers. Langmuir 16: 9421-9432.
- 221. Perez-Luna, V. H., O'Brien, M. J., Opperman, K. A., Hampton, P. D., Lopez, G. P., Klumb, L. A., and Stayton, P. S. (1999) Molecular recognition between genetically engineered streptavidin and surface-bound biotin. J. Am. Chem. Soc. 121: 6469-6478.
- 222. Mann, D. A., Kanai, M., Maly, D. J., and Kiessling, L. L. (1998) Probing low affinity and multivalent interactions with surface plasmon resonance: Ligands for concanavalin A. J. Am. Chem. Soc. 120: 10575-10582.
- 223. Hendrix, M., Priestley, E. S., Joyce, G. F., and Wong, C. (1997) Direct observation of aminoglycoside—RNA interactions by surface plasmon resonance. J. Am. Chem. Soc. 119: 3641–3648.
- 224. Berger, C. E. H., Beumer, T. E. M., Kooyman, R. P. H., and Greve, J. (1998) Surface plasmon resonance multisensing. Anal. Chem. 70: 703-706.
- 225. Brockman, J. M., Frutos, A. G., and Corn, R. M. (1999) A multistep chemical modification procedure to create DNA arrays on gold surfaces for the study of protein-DNA interactions with surface plasmon resonance imaging. J. Am. Chem. Soc. 121: 8044–8051.



- 226. Heaton, R. J., Peterson, A. W., and Georgiadis, R. M. (2001) Electrostatic surface plasmon resonance: Direct electric field-induced hybridization and denaturation in monolayer nucleic acid films and label-free discrimination of base mismatches. Proc. Natl. Acad. Sci. USA 98: 3701-3704.
- 227. Peterson, A. W., Heaton, R. J., and Georgiadis, R. M. (2000) Kinetic control of hybridization in surface immobilized DNA monolayer films. J. Am. Chem. Soc. 122: 7837-7838.
- 228. Jordan, C. E., Frutos, A. G., Thiel, A. J., and Corn, R. M. (1997) Surface plasmon resonance imaging measurements of DNA hybridization adsorption and streptavidin/DNA multilayer formation at chemically modified gold surfaces. Anal. Chem. 69: 4939-4947.
- 229. Nelson, B. P., Grimsrud, T. E., Liles, M. R., Goodman, R. M., and Corn, R. M. (2001) Surface plasmon resonance imaging measurements of DNA and RNA hybridization adsorption onto DNA microarrays. Anal. Chem. 73: 1-7.
- 230. Catalano, S. M., Dodson, E. C., Henze, D. A., Joyce, J. G., Krafft, G. A., and Kinney, G. G. (2006) The role of amyloid-beta derived diffusible ligands (ADDLs) in Alzheimer's disease. Curr. Top. Med. Chem. 6: 597-608.
- 231. Lambert, M. P., Barlow, A. K., Chromy, B. A., Edwards, C., Freed, R., Liosatos, M., Morgan, T. E., Rozovsky, I., Trommer, B., Viola, K. L., Wals, P., Zhang, C., Finch, C. E., Krafft, G. A., and Klein, W. L. (1998) Diffusible, nonfibrillar ligands derived from $A\beta_{1-42}$ are potent central nervous system neurotoxins. Proc. Natl. Acad. Sci. USA 95: 6448-6453.
- 232. Lambert, M. P., Viola, K. L., Chromy, B. A., Chang, L., Morgan, T. E., Yu, J., Venton, D. L., Krafft, G. A., Finch, C. E., and Klein, W. L. (2001) Vaccination with soluble A β oligomers generates toxicity-neutralizing antibodies. J. Neurochem. 79: 595-605.
- 233. Gong, Y., Chang, L., Viola, K. L., Lacor, P. N., Lambert, M. P., Finch, C. E., Krafft, G. A., and Klein, W. L. (2003) Alzheimer's disease-affected brain: Presence of oligomeric A β ligands (ADDLs) suggests a molecular basis for reversible memory loss. Proc. Natl. Acad. Sci. USA 100: 10417-10422.
- 234. Chapman, S. C., Kenny, H. A., and Woodruff, T. K. (2004) Activin, inhihin, and follistatin in ovarian physiology. In The ovary, Leung, P. C. K., and Adashi, E. Y., Eds., Elsevier, San Diego, pp. 273-287.
- 235. Nath, N., and Chilkoti, A. (2002) Immobilized gold nanoparticle sensor for label-free optical detection of biomolecular interactions. Proc. SPIE: Int. Soc. Opt. Eng. 4626: 441-448.
- 236. Nath, N., and Chilkoti, A. (2002) A colorimetric gold nanoparticle sensor to interrogate biomolecular interactions in real time on a surface. Anal. Chem. 74: 504-509.
- 237. Haynes, C. L., and Van Duyne, R. P. (2003) Plasmon-sampled surface-enhanced Raman excitation spectroscopy. Phys. Chem. B 107: 7426-7433.
- 238. Pinchuk, A., Hilger, A., von Plessen, G., and Kreibig, U. (2004) Substrate effect on the optical response of silver nanoparticles. Nanotechnology 15: 1890–1896.
- 239. Wiley, B. J., and Xia, Y. (2005) Localized surface plasmon resonance spectroscopy of single silver nanocubes. Nano Lett. 5: 2034-2038.
- 240. Moskovits, M., and Suh, J. S. (1984) Surface selection rules for surface-enhanced Raman spectroscopy: Calculations and application to the surface-enhanced Raman spectrum of phthalazine on silver. Phys. Chem. 88: 5526-5530.
- 241. Fleischmann, M., Hendra, P. J., and McQuillan, A. J. (1974) Raman spectra of pyridine adsorbed at a silver electrode. Chem. Phys. Lett. 26: 163-166.
- 242. Albrecht, M. G., and Creighton, J. A. (1997) Anomalously intense Raman spectra of pyridine at a silver electrode. *J. Am. Chem. Soc.* 99: 5215–5217.
- 243. Maxwell, D. J., Taylor, J. R., and Nie, S. (2002) Self-assembled nanoparticle probes for recognition and detection of biomolecules. J. Am. Chem. Soc. 124: 9606-9612.
- 244. Sylvia, J. M., Janni, J. A., Klein, J. D., and Spencer, K. M. (2000) Surface-enhanced Raman detection of 2,4-dinitrotoluene impurity vapor as a marker to locate landmines. Anal. Chem. 72:
- 245. Seballos, L., Olson, T. Y., and Zhang, J. Z. (2006) Effects of chromophore orientation and molecule conformation on surface-enhanced Raman scattering studied with alkanoic acids and colloidal silver nanoparticles. Chem. Phys. 125: 234706.



- 246. Seballos, L., Richards, N., Stevens, D. J., Patel, M., Kapitzky, L., Lokey, S., Millhauser, G., and Zhang, J. Z. (2007) Competitive binding effects on surface-enhanced Raman scattering of peptide molecules. Chem. Phys. Lett. 447: 335-339.
- 247. Li, L., Hutter, T., Steiner, U., and Mahajan, S. (2013) Single molecule SERS and detection of biomolecules with a single gold nanoparticle on a mirror junction. Analyst 138: 4574–4578.
- 248. Haran, G. (2010) Single-molecule Raman spectroscopy: A probe of surface dynamics and plasmonic fields. Acc. Chem. Res. 43: 1135-1143.
- 249. Zayak, A. T., Hu, Y. S., Choo, H., Bokor, J., Cabrini, S., Schuck, P. J., and Neaton, J. B. (2011) Chemical Raman enhancement of organic adsorbates on metal surfaces. Phys. Rev. Lett. 106: 083003.
- 250. Le Ru, E. C., Grand, J., Sow, I., Somerville, W. R. C., Etchegoin, P. G., Treguer-Delapierre, M., Charron, G., Felidj, N., Levi, G., and Aubard, J. A. (2011) A scheme for detecting every single target molecule with surface-enhanced Raman spectroscopy. Nano Lett. 11: 5013-5019.
- 251. Moskovits, M. (2005) Surface-enhanced Raman spectroscopy: A brief retrospective. Raman Spectrosc. 36: 485-496.
- 252. Stiles, P. L., Dieringer, F. A., Shah, N. C., and Van Duyne, R. P. (2008) Surface-enhanced Raman spectroscopy. Ann. Rev. Anal. Chem. 1: 601-626.
- 253. Bosnick, K. A., Jiang, J., and Brus, L. E. (2002) Fluctuations and local symmetry in single-molecule rhodamine 6G Raman scattering on silver nanocrystal aggregates. J. Phys. Chem. B 106: 8096-8099.
- 254. Otto, A. I., Morzek, A. I., Grabhorn, H., and Akemann, W. (1992) Surface-enhanced Raman scattering. Phys. Condens. Mater. 4: 1143-1212.
- 255. Aroca, R. (2006) Surface-enhanced vibrational spectroscopy. John Wiley & Sons, Chichester.
- 256. Otto, A. (2005) The 'chemical' (electronic) contribution to surface-enhanced Raman scattering. Raman Spectrosc. 36: 497-509.
- 257. Matveeva, E. G., Gryczynski, I., Barnett, A., Leonenko, Z., Lakowicz, J. R., and Gryczynski, Z. (2007) Metal particle-enhanced fluorescent immunoassays on metal mirrors. Anal. Biochem. 363: 239-245.
- 258. Zhang, J., Fu, Y., Chowdhury, M. H., and Lakowicz, J. R. (2007) Metal-enhanced single-molecule fluorescence on silver particle monomer and dimer: Coupling effect between metal particles. Nano Lett. 7: 2101-2107.
- 259. Zhang, J., Fu, Y., Chowdhury, M. H., and Lakowicz, J. R. (2007) Enhanced Förster resonance energy transfer on single metal particle. 2. Dependence on donor-acceptor separation distance, particle size, and distance from metal surface. Phys. Chem. C 111: 11784-11792.
- 260. Meli, M. V., and Lennox, R. B. (2007) Surface plasmon resonance of gold nanoparticle arrays partially embedded in quartz substrates. Phys. Chem. C 111: 3658-3664.
- 261. Stancu, I. C., Fernandez-Gonzalez, A., and Salzer, R. (2007) SPR imaging antimucin-mucin bioaffinity based biosensor as label-free tool for early cancer diagnosis. Design and detection principle. Opt. Adv. Mater. 9: 1883-1889.
- 262. Ray, K., Szmacinski, H., Enderlein, J., and Lakowicz, J. R. (2007) Distance dependence of surface plasmon-coupled emission observed using Langmuir-Blodgett films. Appl. Phys. Lett. 90: 251116.
- 263. Toderas, F., Baia, M., Baia, L., and Astilean, S. (2007) Controlling gold nanoparticle assemblies for efficient surface-enhanced Raman scattering and localized surface plasmon resonance sensors. Nanotechnology 18: 255702.
- 264. Matveera, E. G., Gryczynski, Z., Malicka, J., Lukomska, J., Makowiec, S., Berndt, K. W., Lakowicz, J. R., and Gryczynski, I. (2005) Directional surface plasmon-coupled emission: Application for an immunoassay in whole blood. Anal. Biochem. 344: 161–167.
- 265. Fu, E., Chinowsky, T., Nelson, K., Johnston, K., Edwards, T., Helton, K., Grow, M., Miller, J. W., and Yager, P. (2007) SPR imaging-based salivary diagnostics system for the detection of small molecule analytes. Ann. NY Acad. Sci. 1098: 335-344.
- 266. Yang, Y., Callahan, J. M., Kim, T. M., Brown, A. S., and Everitt, H. O. (2013) Ultraviolet nanoplasmonics: A demonstration of surface-enhanced Raman spectroscopy, fluorescence, and photodegradation using gallium nanoparticles. Nano Lett. 13: 2837–2841.
- 267. Deckert, V. (2009) Tip-enhanced Raman spectroscopy. Raman Spectrosc. 40: 1336–1337.



- 268. Hall, A. S., Friesen, S. A., and Mallouk, T. E. (2013) Wafer-scale fabrication of plasmonic crystals from patterned silicon templates prepared by nanosphere lithography. Nano Lett. 13: 2623-2627.
- 269. Yeo, B. S., Madler, S., Schmid, T., Zhang, W., and Zenobi, R. (2008) Tip-enhanced Raman spectroscopy can see more: The case of cytochrome C. Phys. Chem. C 112: 4867–4873.
- 270. Satija, J., Punjabi, N. S., Sai, V. V. R., and Mukherji, S. (2014) Optimal design for U-bent fiberoptic LSPR sensor probes. Plasmonics 9: 251-260.
- 271. Srivastava, S. K., Arora, V., Sapra, S., and Gupta, B. D. (2012) Localized surface plasmon resonance-based fiber optic U-shaped biosensor for the detection of blood glucose. Plasmonics 7: 261-268.
- 272. Zhang, S., Wang, N., Yu, H., Niu, Y., and Sun, C. (2005) Covalent attachment of glucose oxidase to an Au electrode modified with gold nanoparticles for use as glucose biosensor. Bioelectro*chemistry* 67: 15–22.
- 273. Verma, R. K., and Gupta, B. D. (2008) Theoretical modelling of a bi-dimensional U-shaped surface plasmon resonance based fibre optic sensor for sensitivity enhancement. Phys. D Appl. Phys. 41: 095106.
- 274. (a) Hsieh, H., Ho, L., and Chang, H. (2016) Aminophenylboronic acid polymer nanoparticles for quantitation of glucose and for insulin release. Anal. Bioanal. Chem. 408: 6557-6565. (b) Wu, W. B., Zhan, L., Jian, W., and Huang, C. Z. (2014) A plasmon resonance light scattering assay of glucose based on the formation of gold nanoparticles. Anal. Methods 6: 3779–3783.
- 275. Dieringer, J. A., McFarland, A. D., Shah, N. C., Stuart, D. A., Whitney, A. V., Yonzon, C. R., Young, M. A., Zhang, X., and Van Duyne, R. P. (2005) Surface enhanced Raman spectroscopy: New materials, concepts, characterization tools, and applications. Faraday Discuss. 132: 9-26.
- 276. Lyandres, O., Shah, N. C., Yonzon, C. R., Walsh, J. T., Glucksberg, M. R., and Van Duyne, R. P. (2005) Real-time glucose sensing by surface-enhanced Raman spectroscopy in bovine plasma facilitated by a mixed decanethiol/mercaptohexanol partition layer. Anal. Chem. 77: 6134-6139.
- 277. Chen, L., Han, X. X., Yang, J. X., Zhou, J., Song, W., Zhao, B., Xu, W. Q., and Ozaki, Y. (2011) Detection of proteins on silica-silver core-shell substrates by surface-enhanced Raman spectroscopy. J. Colloid Interface Sci. 360: 482-487.
- 278. Wang, Y., Wei, H., Li, B., Ren, W., Guo, S. J., Dong, S., and Wang, E. (2007) SERS opens a new way in aptasensor for protein recognition with high sensitivity and selectivity. Chem. Commun. 48: 5220-5225.
- 279. Gong, J. L., Jiang, J. H., Yang, H. F., Shen, G. L., Yu, R. Q., and Ozaki, Y. (2006) Novel dyeembedded core-shell nanoparticles as surface-enhanced Raman scattering tags for immunoassay. *Anal. Chim. Acta* 564: 151–157.
- 280. Sabatte, G., Keir, R., Lawlor, M., Black, M., Graham, D., and Smith, W. E. (2008) Comparison of surface-enhanced resonance Raman scattering and fluorescence for detection of a labeled antibody. Anal. Chem. 80: 2351-2356.
- 281. Pavel, I., McCarney, E., Elkhaled, A., Morrill, A., Plaxco, K., and Moskovits, M. (2008) Label-free SERS detection of small proteins modified to act as bifunctional linkers. Phys. Chem. C: Nanomater. Interfaces 112: 4880-4883.
- 282. Kumar, G. V. P., Reddy, B. A. A., Arif, M., Kundu, T. K., and Narayana, C. (2006) Surfaceenhanced Raman scattering studies of human transcriptional coactivator p300. Phys. Chem. B 110: 16787-16792.
- 283. Feng, M., and Tachikawa, H. (2008) Surface-enhanced resonance Raman spectroscopic characterization of the protein native structure. J. Am. Chem. Soc. 130: 7443–7448.
- 284. Xu, H. X., Bjerneld, E. J., Kall, M., and Borjesson, L. (1999) Spectroscopy of single hemoglobin molecules by surface enhanced Raman scattering. Phys. Rev. Lett. 83: 4357-4360.
- 285. Han, X. X., Cai, L. J., Guo, J., Wang, C. X., Ruan, W. D., Han, W. Y., Xu, W. Q., Zhao, B., and Ozaki, Y. (2008) Fluoresce in isothiocyanate linked immunoabsorbent assay based on surfaceenhanced resonance Raman scattering. Anal. Chem. 80: 3020-3024.
- 286. Cavalu, S., Cinta-Pinzaru, S., Leopold, N., and Kiefer, W. (2001) Raman and surface enhanced Raman spectroscopy of 2,2,5,5-tetramethyl-3-pyrrolin-1-yloxy-3-carboxamide labeled proteins: Bovine serum albumin and cytochrome C. Biopolymers 62: 341-348.

- 287. Han, X. X., Kitahama, Y., Tanaka, Y., Guo, J., Xu, W. Q., Zhao, B., and Ozaki, Y. (2008) Simplified protocol for detection of protein-ligand interactions via surface-enhanced resonance Raman scattering and surface-enhanced fluorescence. Anal. Chem. 80: 6567–6572.
- 288. Han, X. X., Jia, H. Y., Wang, Y. F., Lu, Z. C., Wang, C. X., Xu, W. Q., Zhao, B., and Ozaki, Y. (2008) Analytical technique for label-free multi-protein detection based on western blot and surface-enhanced Raman scattering. Anal. Chem. 80: 2799-2804.
- 289. Tom, R. T., Samal, A. K., Sreeprasad, T. S., and Pradeep, T. (2007) Hemoprotein bioconjugates of gold and silver nanoparticles and gold nanorods: Structure-function correlations. Langmuir 23: 1320-1325.
- 290. Xu, S. P., Ji, X. H., Xu, W. Q., Li, X. L., Wang, L. Y., Bai, Y. B., Zhao, B., and Ozaki, Y. (2004) Immunoassay using probe-labelling immunogold nanoparticles with silver staining enhancement via surface-enhanced Raman scattering. Analyst 129: 63–68.
- 291. Kumar, G. V. P., Shruthi, S., Vibha, B., Reddy, B. A. A., Kundu, T. K., and Narayana, C. (2007) Hot spots in Ag core-Au shell nanoparticles potent for surface-enhanced Raman scattering studies of biomolecules. Phys. Chem. C 111: 4388–4392.
- 292. Penn, M. A., Drake, D. M., and Driskell, J. D. (2013) Accelerated surface-enhanced Raman spectroscopy (SERS)-based immunoassay on a gold-plated membrane. Anal. Chem. 85: 8609-8617.
- 293. Cui, Y., Ren, B., Yao, J. L., Gu, R. A., and Tian, Z. Q. (2006) Synthesis of Ag_{core}Au_{shell} bimetallic nanoparticles for immunoassay based on surface-enhanced Raman spectroscopy. Phys. Chem. B 110: 4002-4006.
- 294. Singh, P., Thuy, N. T. B., Aoki, Y., Mott, D., and Maenosono, S. (2011) Intensification of surface enhanced Raman scattering of thiol-containing molecules using Ag@Au core@ shell nanoparticles. Appl. Phys. 109(9): 094301-1-094301-7.
- 295. Gopinath, A., Boriskina, S. V., Reinhard, B. M., and Negro, L. D. (2009) Deterministic aperiodic arrays of metal nanoparticles for surface-enhanced Raman scattering (SERS). Opt. Express 17: 3741-3753.
- 296. Gellini, C., Muniz-Miranda, M., Innocenti, M., Carlà, F., Loglio, F., Foresti, M. L., and Salvi, P. R. (2008) Nanopatterned Ag substrates for SERS spectroscopy. Phys. Chem. Chem. Phys. 10: 4555-
- 297. Chithrani, B. D., and Chan, W. C. W. (2007) Elucidating the mechanism of cellular uptake and removal of protein-coated gold nanoparticles of different sizes and shapes. Nano Lett. 7: 1542-1550.
- 298. Kneipp, K., Haka, A. S., Kneipp, H., Badizadegan, K., Yoshizawa, N., Boone, C., Shafer-Peltier, K. E., Motz, J. T., Dasari, R. R., and Feld, M. S. (2002) Surface-enhanced Raman spectroscopy in single living cells using gold nanoparticles. Appl. Spectrosc. 56: 150-154.
- 299. Ko, J., Lee, S., Lee, E. K., Chang, S. I., Chen, L., Yoon, S. Y., and Choo, J. (2013) Highly sensitive SERS-based immunoassay of aflatoxin B1 using silica-encapsulated hollow gold nanoparticles. Phys. Chem. Chem. Phys. 15: 5379-5385.
- 300. Kneipp, J., Kneipp, H., and Kneipp, K. (2006) Two-photon vibrational spectroscopy for biosciences based on surface-enhanced hyper-Raman scattering. Proc. Natl. Acad. Sci. USA 103: 17149-
- 301. Schwartzberg, A. M., Oshiro, T. Y., Zhang, J. Z., Huser, T., and Talley, C. E. (2006) Improving nanoprobes using surface-enhanced Raman scattering from 30-nm hollow gold particles. Anal. Chem. 78: 4732-4736.
- 302. Mahmoud, M. A., O'Neil, D., and El-Sayed, M. A. (2014) Hollow and solid metallic nanoparticles in sensing and in nanocatalysis. Chem. Mater. 26: 44–58.
- 303. Jahn, M., Patze, S., Bocklitz, T., Weber, K., Cialla-May, D., and Popp, J. (2015) Towards SERS based applications in food analytics: Lipophilic sensor layers for the detection of Sudan III in food matrices. Anal. Chim. Acta 860: 43-50.
- 304. Ou, X., Tan, X., Wei, S., Chen, S., Zhang, J., and Liu, X. (2014) Electrochemiluminescence biosensor for cholesterol detection based on AuNPs/L-cys-C₆₀ nanocomposites. Anal. Methods 6: 3804-3810.



- 305. Noor, M. O., and Krull, U. J. (2014) Silicon nanowires as field-effect transducers for biosensor development: A review. Anal. Chim. Acta 825: 1-25.
- 306. Estevez, M.-C., Otte, M. A., Sepulveda, B., and Lechuga, L. M. (2014) Trends and challenges of refractometric nanoplasmonic biosensors: A review. Anal. Chim. Acta. 806: 55-73.
- 307. Hall, D. (2001) Use of optical biosensors for the study of mechanistically concerted surface adsorption processes. Anal. Biochem. 288: 109-125.
- 308. Wolterbeek, H. T., and Van Der Meer, A. J. G. M. (1996) A sensitive and quantitative biosensing method for the determination of γ -ray emitting radionuclides in surface water. Environ. Radioact. 33: 237-254.
- 309. Wang, J., Cai, X., Rivas, G., Shiraishi, H., Farias, P. A., and Dontha, N. (1996) DNA electrochemical biosensor for the detection of short DNA sequences related to the human immunodeficiency virus. Anal. Chem. 68: 2629-2634.
- 310. Thevenot, D. R., Toth, K., Durst, R. A., and Wilson, G. S. (2001) Electrochemical biosensors: Recommended definitions and classification. Biosens. Bioelectron. 16: 121-131.
- 311. Mascini, M., Palchetti, I., and Marrazza, G. (2001) DNA electrochemical biosensors. Fresenius J. Anal. Chem. 369: 15-22.
- 312. Bi, L., Dong, J., Xie, W., Lu, W., Tong, W., Tao, L., and Qian, W. (2013) Bimetallic gold-silver nanoplate array as a highly active SERS substrate for detection of streptavidin/biotin assemblies. Anal. Chim. Acta 805: 95-100.
- 313. Horacek, J., and Skladal, P. (1997) Improved direct piezoelectric biosensors operating in liquid solution for the competitive label-free immunoassay of 2,4-dichlorophenoxyacetic acid. Anal. *Chim. Acta* 347: 43–50.
- 314. Ebersole, R. C., Miller, J. A., Moran, J. R., and Ward, M. D. (1990) Spontaneously formed functionally active avidin monolayers on metal surfaces: A strategy for immobilizing biological reagents and design of piezoelectric biosensors. J. Am. Chem. Soc. 112: 3239-3341.
- 315. Miller, M. M., Sheehan, P. E., Edelstein, R. L., Tamanaha, C. R., Zhong, L. S., Bounnak, L., Whitman, J. L., and Colton, R. J. (2001) A DNA array sensor utilizing magnetic microbeads and magnetoelectronic detection. J. Magn. Magn. Mater. 225: 138-144.
- 316. Chemla, Y. R., Grossman, H. L., Poon, Y., McDermott, R., Stevens, R., Alper, M. D., and Clarke, J. (2000) Ultrasensitive magnetic biosensor for homogeneous immunoassay. Proc. Natl. Acad. Sci. USA 97: 14268-14272.
- 317. Natsume, T., Nakayama, H., and Isobe, T. (2001) BIA-MS-MS: Biomolecular interaction analysis for functional proteomics. Trends Biotechnol. 19: S28–S33.
- 318. Yeo, B. S., Stadler, J., Schmid, T., Zenobi, R., and Zhang, W. (2009) Tip-enhanced Raman spectroscopy - Its status, challenges and future directions. Chem. Phys. Lett. 472: 1-13.
- 319. Polla, D. L., Erdman, A. G., Robbins, W. P., Markus, D. T., Diaz-Diaz, J., Rizq, R., Nam, Y., Brickner, H. T., Wang, A., and Krulevitch, P. (2000) Microdevices in medicine. Annu. Rev. Biomed. Eng. 2: 551-576.
- 320. Stockle, R. M., Suh, Y. D., Deckert, V., and Zenobi, R. (2000) Nanoscale chemical analysis by tipenhanced Raman spectroscopy. Chem. Phys. Lett. 318: 131-136.
- 321. Hayazawa, N., Inouye, Y., Sekkat, Z., and Kawata, S. (2000) Metallized tip amplification of nearfield Raman scattering. Opt. Commun. 183: 333-336.
- 322. Anderson, M. S. (2000) Locally enhanced Raman spectroscopy with an atomic force microscope. Appl. Phys. Lett. 76: 3130-3132.
- 323. Weber-Bargioni, A., Schwartzberg, A., Cornaglia, M., Ismach, A., Urban, J. J., Pang, Y., Gordon, R., Bokor, J., Salmeron, M. B., Ogletree, D. F., Ashby, P., Cabrini, S., and Schuck, P. J. (2011) Hyperspectral nanoscale imaging on dielectric substrates with coaxial optical antenna scan probes. Nano Lett. 11: 1201-1207.
- 324. Berweger, S., Neacsu, C. C., Mao, Y. B., Zhou, H. J., Wong, S. S., and Raschke, M. B. (2009) Optical nanocrystallography with tip-enhanced phonon Raman spectroscopy. Nat. Nanotechnol. 4:
- 325. Roth, R. M., Panoiu, N. C., Adams, M. M., Osgood, R. M., Neacsu, C. C., and Raschke, M. B. (2006) Resonant-plasmon field enhancement from asymmetrically illuminated conical metallicprobe tips. Opt. Express 14: 2921–2931.

- 326. Andersson, O., Ulrich, C., Bjorefors, F., and Liedberg, B. (2008) Imaging SPR for detection of local electrochemical processes on patterned surfaces. Sensors Actuat. B: Chem. 134: 545-550.
- 327. Anderson, N., Hartschuh, A., and Novotny, L. (2007) Chirality changes in carbon nanotubes studied with near-field Raman spectroscopy. Nano Lett. 7: 577-582.
- 328. Anderson, N., Anger, P., Hartschuh, A., and Novotny, L. (2006) Subsurface Raman imaging with nanoscale resolution. Nano Lett. 6: 744-749.
- 329. Pettinger, B., Ren, B., Picardi, G., Schuster, R., and Ertl, G. (2004) Nanoscale probing of adsorbed species by tip-enhanced Raman spectroscopy. Phys. Rev. Lett. 92: 096101.
- 330. Neacsu, C. C., Dreyer, J., Behr, N., and Raschke, M. B. (2006) Scanning-probe Raman spectroscopy with single-molecule sensitivity. Phys. Rev. B 73: 193406.
- 331. Domke, K. F., Zhang, D., and Pettinger, B. (2006) Toward Raman fingerprints of single dye molecules at atomically smooth Au(III). J. Am. Chem. Soc. 128: 14721-14727.
- 332. Zhang, X., Zhao, J., Whiteney, A. V., Elam, J. W., and Van Duyne, R. P. (2006) Ultrastable substrates for surface-enhanced Raman spectroscopy: Al₂O₃ overlayers fabricated by atomic layer deposition yield improved anthrax biomarker detection. J. Am. Chem. Soc. 128: 10304-10309.
- 333. Zhang, W., Yeo, B. S., Schmid, T., and Zenobi, R. (2007) Single molecule tip-enhanced Raman spectroscopy with silver tips. *Phys. Chem. C* 111: 1733–1738.
- 334. Zhang, X., Young, M. A., Lyandres, O., and Van Duyne, R. P. (2005) Rapid detection of an anthrax biomarker by surface-enhanced Raman spectroscopy. J. Am. Chem. Soc. 127: 4484-4489.
- 335. Saptarshi, S. R., Duschl, A., and Lopata, A. L. (2013) Interaction of nanoparticles with proteins: Relation to bio-reactivity of the nanoparticle. J. Nanobiotechnol. 11: 26.
- 336. Lakowicz, J. R. (2006) Plasmonics in biology and plasmon-controlled fluorescence. Plasmonics 1: 5-33.
- 337. Hanken, D. G., Jordan, C. E., Frey, B. L., and Corn, R. M. (1998) Surface plasmon resonance measurements of ultrathin organic films at electrode surfaces. Electroanal. Chem. 20: 141-225.
- 338. Gartia, M. R., Lu, M., and Liu, G. L. (2013) Surface plasmon coupled whispering gallery mode for guided and free-space electromagnetic waves. Plasmonics 8: 361-368.
- 339. Brar, V. W., Jang, M. S., Sherrott, M., Lopez, J. J., and Atwater, H. A. (2013) Highly confined tunable mid-infrared plasmonics in graphene nanoresonators. Nano Lett. 13: 2541-2547.
- 340. Ghoshal, A., and Kik, P. G. (2008) Theory and simulation of surface plasmon excitation using resonant metal nanoparticle arrays. Appl. Phys. 103: 113111.
- 341. Horvath, H. J. (2009) Gustav Mie and the scattering and absorption of light by particles: Historic developments and basics. Quant. Spectrosc. Radiat. Transf. 110: 787–799.
- 342. Norman, T. J., Grant, C. D., Magana, D., Zhang, J. Z., Liu, J., Cao, D., Bridges, F., and Buuren, A. V. (2002) Near infrared optical absorption of gold nanoparticle aggregates. Phys. Chem. B 106: 7005-7012.
- 343. Murphy, C. J., Sau, T. K., Gole, A. M., Orendorff, C. J., Gao, J., Gou, L., Hunyadi, S., and Li, T. (2005) Anisotropic metal nanoparticles: Synthesis, assembly, and optical applications. Phys. *Chem. B* 109: 13857–13870.
- 344. Gou, L. F., and Murphy, C. J. (2005) Fine-tuning the shape of gold nanorods. Chem. Mater. 17: 3668-3672.
- 345. Murphy, C. J., Sau, T. K., Gole, A., and Orendroff, C. J. (2005) Surfactant-directed synthesis and optical properties of one-dimensional plasmonic nanostructures. MRS Bull. 30: 349-355.
- 346. Mahmoud, M. A., and El-Sayed, M. A. (2013) Different plasmon sensing behavior of silver and gold nanorods. Phys. Chem. Lett. 4: 1541-1545.
- 347. Sun, Y. G., Mayers, B. T., and Xia, Y. N. (2002) Template-engaged replacement reaction: A onestep approach to the large-scale synthesis of metal nanostructures with hollow interiors. Nano Lett. 2: 481-485.
- 348. Sun, Y. G., Mayers, B., and Xia, Y. N. (2003) Transformation of silver nanospheres into nanobelts and triangular nanoplates through a thermal process. *Nano Lett.* 3: 675–679.



- 349. Schwartzberg, A. M., Olson, T. Y., Talley, C. E., and Zhang, J. Z. (2006) Synthesis characterization, and tunable optical properties of hollow gold nanospheres. Phys. Chem. B 110: 19935-19944.
- 350. Schwartzberg, A. M., Grant, C. D., van Buuren, T., and Zhang, J. Z. (2007) Reduction of HAuCl₄ by Na₂S revisited: The case for Au nanoparticle aggregates and against Au₂S/Au core/shell particles. Phys. Chem. C 111: 8892-8901.
- 351. Yi, F., Zhu, H., Reed, J. C., and Cubukcu, E. (2013) Plasmonically enhanced thermomechanical detection of infrared radiation. Nano Lett. 13: 1638-1643.
- 352. Oyelere, A. K., Chen, P. C., Huang, X., El-Sayed, I. H., and El-Sayed, M. A. (2007) Peptide-conjugated gold nanorods for nuclear targeting. *Bioconjugate Chem.* 18: 1490–1497.
- 353. Jain, P. K., Huang, X., El-Sayed, I. H., and El-Sayed, M. A. (2007) Review of some interesting surface plasmon resonance-enhanced properties of noble metal nanoparticles and their applications to biosystems. Plasmonics 2: 107-118.
- 354. Huang, X., Jain, P. K., El-Sayed, I. H., and El-Sayed, M. A. (2007) Special focus: Nanoparticles for cancer diagnosis & therapeutics - Review. Nanomedicine 2: 681-693.
- 355. El-Sayed, I. H., Huang, X., and El-Sayed, M. A. (2006) Selective laser photo-thermal therapy of epithelial carcinoma using anti-EGFR antibody conjugated gold nanoparticles. Cancer Lett. 239: 129-135.
- 356. Lin, J., Wang, S., Huang, P., Wang, Z., Chen, S., Niu, G., Li, W., He, J., Cui, D., Lu, G., Chen, X., and Nie, Z. (2013) Photosensitizer-loaded gold vesicles with strong plasmonic coupling effect for imaging-guided photothermal/photodynamic therapy. ACS Nano 7: 5320–5329.
- 357. Melancon, M. P., Lu, W., Yang, Z., Zhang, R., Cheng, Z., Elliot, A. M., Stafford, J., Olson, T., Zhang, J. Z., and Li, C. (2008) In vitro and in vivo targeting of hollow gold nanoshells directed at epidermal growth factor receptor for photothermal ablation therapy. Mol. Cancer Ther. 7: 1730-
- 358. Loo, C., Lin, A., Hirsch, L., Lee, M. H., Barton, J., Halas, N., West, J., and Drezek, R. (2004) Nanoshell-enabled photonics-based imaging and therapy of cancer. Technol. Cancer Res. Treat. 3: 33-40.
- 359. Ploman, A. (2008) Plasmonics applied. Science 322: 868-869.
- 360. George, S. M. (2010) Atomic layer deposition: An overview. Chem. Rev. 110: 111-131.
- 361. Wolden, C. A., Kurtin, J., Baxter, J. B., Repins, I., Shaheen, S. E., Torvik, J. T., Rockett, A. A., Fthenakis, V. M., and Aydil, E. S. (2011) Photovoltaic manufacturing: Present status, future prospects, and research needs. Vac. Sci. Technol. A 29: 030801.
- 362. Lin, J., Mueller, J. P. B., Wang, Q., Yuan, G., Antoniou, N., Yuan, X. C., and Capasso, F. (2013) Polarization-controlled tunable directional coupling of surface plasmon polaritons. Science 340: 331-334.
- 363. Lindquist, N. C., Nagpal, P., McPeak, K. M., Norris, D. J., and Oh, S. H. (2012) Engineering metallic nanostructures for plasmonics and nanophotonics. Rep. Prog. Phys. 75: 036501.
- 364. Stuart, H. R., and Hall, D. G. (1996) Enhanced dipole-dipole interaction between elementary radiators near a surface. Phys. Rev. Lett. 80: 5663-5666.
- 365. Schaadt, D. M., Feng, B., and Yu, E. T. (2005) Enhanced semiconductor optical absorption via surface plasmon excitation in metal nanoparticles. Appl. Phys. Lett. 86: 063106.
- 366. Nakayama, K., Tanabe, K., and Atwater, H. A. (2008) Plasmonic nanoparticle enhanced light absorption in GaAs solar cells. Appl. Phys. Lett. 93: 121904.
- 367. Qu, D., Liu, F., Yu, J., Xie, W., Xu, Q., Li, X., and Huang, Y. (2011) Plasmonic core-shell gold nanoparticle enhanced optical absorption in photovoltaic devices. Appl. Phys. Lett. 98: 113119.
- 368. Pryce, I. M., Koleske, D. D., Fischer, A. J., and Atwater, H. A. (2010) Plasmonic nanoparticle enhanced photocurrent in GaN/InGaN/GaN quantum well solar cells. Appl. Phys. Lett. 96: 153501.
- 369. Chen, F. C., Wu, J. L., Lee, C. L., Hong, Y., Kuo, C. H., and Huang, M. H. (2009) Plasmonicenhanced polymer photovoltaic devices incorporating solution-processable metal nanoparticles. Appl. Phys. Lett. 95: 013305.

- 370. Derkacs, D., Chen, W. V., Matheu, P. M., Lim, S. H., Yu, P. K. L., and Yu, E. T. (2008) Nanoparticle-induced light scattering for improved performance of quantum-well solar cells. Appl. Phys. Lett. 93: 091107.
- 371. Derkacs, D., Lim, S. H., Matheu, P., Mar, W., and Yu, E. T. (2006) Improved performance of amorphous silicon solar cells via scattering from surface plasmon polaritons in nearby metallic nanoparticles. Appl. Phys. Lett. 89: 093103.
- 372. Bohren, C. F. (1983) How can a particle absorb more than the light incident on it? Am. J. Phys. 51: 323–327.
- 373. Mertz, J. (2000) Radiative absorption, fluorescence, and scattering of a classical dipole near a lossless interface: A unified description. Opt. Soc. Am. B 17: 1906–1913.
- 374. Atwater, H. A., and Polman, A. (2010) Plasmonics for improved photovoltaic devices. Nat. Mater. 9: 205-213.
- 375. Spinelli, P., Hebbink, M., de Waele, R., Black, L., Lenzmann, F. O., and Polman, A. (2011) Optical impedance matching using coupled plasmonic nanoparticle arrays. Nano Lett. 11: 1760–1765.
- 376. Beck, F. J., Polman, A., and Catchpole, K. R. (2009) Tunable light trapping for solar cells using localized surface plasmons. Appl. Phys. 105: 114310.
- 377. Ferry, V. E., Verschuuren, M. A., Li, H. B. T., Verhagen, E., Walters, R. J., Schropp, R. E. I., Atwater, H. A., and Polman, A. (2010) Light trapping in ultrathin plasmonic solar cells. Opt. Express 18: A237-A245.
- 378. Renger, J., Grafstrom, S., and Eng, L. M. (2007) Direct excitation of surface plasmon polaritons in nanopatterned metal surfaces and thin films. Phys. Rev. B 76: 045431.
- 379. Andkjær, J., Nishiwaki, S., Nomura, T., and Sigmund, O. (2010) Topology optimization of grating couplers for the efficient excitation of surface plasmons. Opt. Soc. Am. B 27: 1828–1832.
- 380. Haug, F., Soderstrom, T., Cubero, O., Daudrix, V. T., and Ballif, C. (2008) Plasmonic absorption in textured silver back reflectors of thin film solar cells. Appl. Phys. 104: 064509.
- 381. Zhu, J., Hsu, C. M., Yu, Z., Fan, S., and Cui, Y. (2010) Nanodome solar cells with efficient light management and self-cleaning. Nano Lett. 10: 1979-1984.
- 382. Wang, J. Y., Tsai, F. J., Huang, J. J., Chen, C. Y., Li, N., Kiang, Y. W., and Yang, C. C. (2010) Enhancing InGaN-based solar cell efficiency through localized surface plasmon interaction by embedding Ag nanoparticles in the absorbing layer. Opt. Express 18: 2682–2694.
- 383. Abdulhalim, I., Zourob, M., and Lakhtakia, A. (2008) Surface plasmon resonance for biosensing: A mini-review. *Electromagnetics* 28: 214–242.
- 384. Shankaran, D. R., Gobi, K. V., and Miura, N. (2007) Recent advancements in surface plasmon resonance immunosensors for detection of small molecules of biomedical, food and environmental interest. Sensors Actuat. B: Chem. 121: 158–177.
- 385. Myszka, D. G., and Rich, R. L. (2000) Implementing surface plasmon resonance biosensors in drug discovery. Pharma. Sci. Technolo. Today 3: 310-317.
- 386. Homala, J. (2003) Present and future of surface plasmon resonance biosensors. Anal. Bioanal. Chem. 377: 528-539.
- 387. Tudos, A. J., van den Bos, E. R. L., and Stigter, E. C. A. (2003) Rapid surface plasmon resonancebased inhibition assay of deoxynivalenol. J. Agric. Food Chem. 51: 5843-5848.
- 388. Qu, F., Zhou, X., Xu, J., Li, H., and Xie, G. (2009) Luminescence switching of CdTe quantum dots in presence of p-sulfonatocalix[4] arene to detect pesticides in aqueous solution. Talanta 78: 1359-1363.
- 389. Funari, R., Ventura, B. D., Schiavo, L., Esposito, R., Altucci, C., and Velotta, R. (2013) Detection of parathion pesticide by quartz crystal microbalance functionalized with UV-activated antibodies. Anal. Chem. 85: 6392-6397.
- 390. Multari, R. A., Cremers, D. A., Scott, T., and Kendrick, P. (2013) Detection of pesticides and dioxins in tissue fats and rendering oils using laser-induced breakdown spectroscopy (LIBS). J. Agric. Food Chem. 61: 2348-2357.
- 391. Lee, E. H., Kim, Y. A., Lee, Y. T., Hammock, B. D., and Lee, H. S. (2013) Competitive immunochromatographic assay for the detection of the organophosphorus pesticide EPN. Food Agric. Immunol. 24: 129-138.



- 392. Mauriz, E., Calle, A., Lechuga, L. M., Quintana, J., Montoya, A., and Manclus, J. J. (2006) Realtime detection of chlorpyrifos at part per trillion levels in ground, surface and drinking water samples by a portable surface plasmon resonance immunosensor. Anal. Chim. Acta 561: 40–47.
- 393. Shimomura, M., Nomura, Y., Zhang, W., Sakino, M., Lee, K., Ikebukuro, K., and Karube, I. (2001) Simple and rapid detection method using surface plasmon resonance for dioxins, polychlorinated biphenylx and atrazine. Anal. Chim. Acta 434: 223-230.
- 394. Khan, A. A., and Akhtar, T. (2011) Adsorption thermodynamics studies of 2,4,5-trichlorophenoxy acetic acid on poly-o-toluidine Zr(IV) phosphate, a nano-composite used as pesticide sensitive membrane electrode. Desalination 272: 259-264.
- 395. Kuang, H., Chen, W., Yan, W. J., Xu, L. G., Zhu, Y. Y., Liu, L. Q., Chu, H. Q., Peng, C. F., Wang, L. B., Kotov, N. A., and Xu, C. L. (2011) Crown ether assembly of gold nanoparticles: Melamine sensor. Biosens. Bioelectron. 26: 2032–2037.
- 396. Sun, H., and Fung, Y. (2006) Piezoelectric quartz crystal sensor for rapid analysis of pirimicarb residues using molecularly imprinted polymers as recognition elements. Anal. Chim. Acta 576: 67-76.
- 397. Parham, H., and Rahbar, N. (2010) Square wave voltammetric determination of methyl parathion using ZrO₂-nanoparticles modified carbon paste electrode. J. Hazard. Mater. 177: 1077–1084.
- 398. Zhao, Y., Zhang, W., Lin, Y., and Du, D. (2013) The vital function of Fe₃O₄@Au nanocomposites for hydrolase biosensor design and its application in detection of methyl parathion. Nanoscale 5: 1121-1126.
- 399. Navarro, P., Perez, A. J., Gabaldon, J. A., Delicado, E. N., Puchades, R., Maquieira, A., and Morais, S. (2013) Detection of chemical residues in tangerine juices by a duplex immunoassay. Talanta 116: 33-38.
- 400. Tankiewicz, M., Morrison, C., and Biziuk, M. (2013) Multi-residue method for the determination of 16 recently used pesticides from various chemical groups in aqueous samples by using DI-SPME coupled with GC-MS. Talanta 107: 1-10.
- 401. Lin, T. J. K., Huang, T., and Liu, C. Y. (2006) Determination of organophosphorous pesticides by a novel biosensor based on localized surface plasmon resonance. Biosens. Bioelectron. 22: 513-518.
- 402. Leonard, P., Hearty, S., Quinn, J., and Kennedy, R. O. (2004) A generic approach for the detection of whole Listeria monocytogenes cells in contaminated samples using surface plasmon resonance. Biosens. Bioelectron. 19: 1331-1335.
- 403. Miyajima, K., Koshida, T., Arakawa, T., Kudo, H., Saito, H., Yano, K., and Mitsubayashi, K. (2013) Fiber-optic fluoroimmunoassay system with a flow-through cell for rapid on-site determination of Escherichia coli O157:H7 by monitoring fluorescence dynamics. Biosensors 3: 120–131.
- 404. dos Santos, M. B., Agusil, J. P., Prieto-Simon, B., Sporer, C., Teixeira, V., and Samitier, J. (2013) Highly sensitive detection of pathogen Escherichia coli O157:H7 by electrochemical impedance spectroscopy. Biosens. Bioelectron. 45: 174-180.
- 405. Subramanian, A., Irudayaraj, J., and Ryan, T. (2006) A mixed self-assembled monolayer-based surface plasmon immunosensor for detection of E. coli O157:H7. Biosens. Bioelectron. 21: 998-1006.
- 406. Meeusen, C. A., Alocilja, E. C., and Osburn, W. N. (2005) Detection of E. coli O157:H7 using a miniaturized surface plasmon resonance biosensor. Trans. Am. Soc. Agric. Eng. 6: 2409-2416.
- 407. Oh, B. K., Lee, W., Chun, B. S., Bae, Y. M., Lee, W. H., and Choi, J. W. (2005) Surface plasmon resonance immunosensor for the detection of Yersinia enterocolitica. Colloids Surf. A 257–258: 369–374.
- 408. De Lorenzis, E., Manera, M. G., Montagna, G., Cimaglia, F., Chiesa, M., Poltronieri, P., Santino, A., and Rella, R. (2013) Erratum to 'SPR based immunosensor for detection of Legionella pneumophila in water samples. Opt. Commun. 294: 420–426.
- 409. Tawil, N., Mouawad, F., Levesque, S., Sacher, E., Mandeville, R., and Meunier, M. (2013) The differential detection of methicillin-resistant, methicillin-susceptible and borderline oxacillin-resistant Staphylococcus aureus by surface plasmon resonance. Biosens. Bioelectron. 49: 334-340.
- 410. Wei, D., Oyarzabal, O. A., Huang, T. S., Balasubramanian, S., Sista, S., and Simonian, A. L. (2007) Development of a surface plasmon resonance biosensor for the identification of Campylobacter jejuni. Microbiol. Methods 69: 78-85.



- 411. Hearty, S., Leonard, P., Quinn, J., and O'Kennedy, R. (2006) Production, characterisation and potential application of a novel monoclonal antibody for rapid identification of virulent Listeria monocytogenes. Microbiol. Methods 66: 294-312.
- 412. Jyoung, J. Y., Hong, S., Lee, W., and Choi, J. W. (2006) Immunosensor for the detection of Vibrio cholerae O1 using surface plasmon resonance. Biosens. Bioelectron. 21: 2315-2319.
- 413. Charlermroj, R., Oplatowska, M., Gajanandana, O., Himananto, O., Grant, I. R., Karoonuthaisiri, N., and Elliott, C. T. (2013) Strategies to improve the surface plasmon resonance-based immmunodetection of bacterial cells. Microchim. Acta 180: 643-650.
- 414. Jiang, D., Ji, J., An, L., Sun, X., Zhang, Y., Zhang, G., and Tang, L. (2013) Mast cell-based electrochemical biosensor for quantification of the major shrimp allergen Pen a 1 (tropomyosin). Biosens. Bioelectron. 50: 150-156.
- 415. Ahu, S., Freedman, D. S., Massari, P., Cabodi, M., and Unlu, M. S. (2013) A mass-tagging approach for enhanced sensitivity of dynamic cytokine detection using a label-free biosensor. Langmuir 29: 5369-5376.
- 416. Muller-Renaud, S., Dupont, D., and Dulieu, P. (2004) Quantification of β -casein in milk and cheese using an optical immunosensor. J. Agric. Food. Chem. 52: 659-664.
- 417. Mohammed, I., Mullett, W. M., Lai, E. P. C., and Yeung, J. M. (2001) Is biosensor a viable method for food allergen detection? Anal. Chim. Acta 444: 97-102.
- 418. Lalla, C. D., Tamborini, E., Longhi, R., Tresoldi, E., Manoni, M., Siccardi, A. G., Arosio, P., and Sidoli, A. (1996) Human recombinant antibody fragments specific for a rye-grass pollen allergen: Characterization and potential applications. *Mol. Immunol.* 33: 1049–1058.
- 419. Li, Y., Kobayashi, M., Furui, K., Soh, N., Nakano, K., and Imato, T. (2006) Surface plasmon resonance immunosensor for histamine based on an indirect competitive immunoreaction. Anal. *Chim. Acta* 576: 77–83.
- 420. Vaisocherova, H., Mrkvova, K., Piliarik, M., Jinoch, P., Steinbachova, M., and Homola, I. (2007) Surface plasmon resonance biosensor for direct detection of antibody against Epstein-Barr virus. Biosens. Bioelectron. 22: 1020-1026.
- 421. Zeng, C., Huang, X., Xu, J., Li, G., Ma, J., Ji, H. F., Zhu, S., and Chen, H. (2013) Rapid and sensitive detection of maize chlorotic mottle virus using surface plasmon resonance-based biosensor. Anal. Biochem. 440: 18-22.
- 422. Wang, X., Chen, L., Su, X., and Ai, S. (2013) Electrochemical immunosensor with graphene quantum dots and apoferritin-encapsulated Cu nanoparticles double-assisted signal amplification for detection of avian leukosis virus subgroup. J. Biosens. Bioelectron. 47: 171-177.
- 423. Lu, X., Dong, X., Zhang, K., Han, X., Fang, X., and Zhang, Y. (2013) A gold nanorods-based fluorescent biosensor for the detection of hepatitis B virus DNA based on fluorescence resonance energy transfer. Analyst 138: 642-650.
- 424. Li, M., Cushing, S. K., Liang, H., Suri, S., Ma, D., and Wu, N. (2013) Plasmonic nanorice antenna on triangle nanoarray for surface-enhanced Raman scattering detection of hepatitis B virus DNA. Anal. Chem. 85: 2072-2078.
- 425. Ymeti, A., Greve, J., Lambeck, P. V., Wink, T., Stephan, W. F. M., Tom, A. M., Wijn, R. R., Heideman, R. G., Subramaniam, V., and Kanger, J. S. (2007) Fast, ultrasensitive virus detection using a young interferometer sensor. Nano Lett. 7: 394–397.